# Emissions of trace gases and aerosols during the open combustion of biomass in the laboratory

Gavin R. McMeeking[1,2*], Sonia M. Kreidenweis[1], Stephen Baker[3], Christian M. Carrico[1], Judith C. Chow[4], Jeffrey L. Collett, Jr.[1], Wei Min Hao[3], Amanda S. Holden[1], Thomas W. Kirchstetter[5], William C. Malm[6], Hans Moosmüller[4], Amy P. Sullivan[1], and Cyle E. Wold[3]

[1]Department of Atmospheric Science, Colorado State University, Fort Collins, Colorado, USA

[2]Now at Center for Atmospheric Science, University of Manchester, Manchester, UK

[3]Fire Sciences Laboratory, United States Forest Service, Missoula, Montana, USA

[4]Division of Atmospheric Sciences, Desert Research Institute, Nevada System of Higher Education, Reno, Nevada, USA

[5]Environmental Energy Technologies Division, Lawrence Berkeley National Laboratory, Berkeley, California, USA

[6]National Park Service/CIRA, Colorado State University, Fort Collins, Colorado, USA

*To whom correspondence should be addressed, gavin.mcmeeking@manchester.ac.uk

Submitted to: Journal of Geophysical Research – Atmospheres

15 May 2009

## ABSTRACT

We characterized the gas- and speciated aerosol-phase emissions from the open combustion of 33 different plant species during a series of 255 controlled laboratory burns during the Fire Laboratory at Missoula Experiments (FLAME). The plant species we tested were chosen to improve the existing database for U.S. domestic fuels: laboratory-based emission factors have not previously been reported for many commonly-burned species that are frequently consumed by fires near populated regions and protected scenic areas. The plants we tested included the chaparral species chamise, manzanita, and ceanothus, and species common to the southeastern US (common reed, hickory, kudzu, needlegrass rush, rhododendron, cord grass, sawgrass, titi, and wax myrtle). Fire-integrated emission factors for gas-phase $CO_2$, $CO$, $CH_4$, $C_{2-4}$ hydrocarbons, $NH_3$, $SO_2$, $NO$, $NO_2$, $HNO_3$ and particle-phase organic carbon (OC), elemental carbon (EC), $SO_4^{2-}$, $NO_3^-$, $Cl^-$, $Na^+$, $K^+$, and $NH_4^+$ generally varied with both fuel type and with the fire-integrated modified combustion efficiency (MCE), a measure of the relative importance of flaming- and smoldering-phase combustion to the total emissions during the burn. Chaparral fuels tended to emit less particulate OC per unit mass of dry fuel than did other fuel types, whereas southeastern species had some of the largest observed EF for total fine particulate matter. Our measurements often spanned a larger range of MCE than prior studies, and thus help to improve estimates for individual fuels of the variation of emissions with combustion conditions.



## INDEX TERMS

aerosols and particles (0305), constituent sources and sinks (0322), geochemical cycles (0330), pollution: urban and regional (0345), biogeochemical cycles (0414), biosphere/atmosphere

41 interactions (0315)

42 1. INTRODUCTION

43 Biomass burning emissions are a significant, global source of trace gas and aerosol
44 species in the atmosphere and affect climate, visibility and human health [*Crutzen and Andreae*,
45 1990; *Naeher et al.*, 2007; *Watson*, 2002]. Although biomass burning emissions in the
46 continental United States have been estimated to represent only ~5% of annual average global
47 emissions (computed for 1997-2004) [*van der Werf et al.*, 2006], they play a large role in U.S.
48 urban and regional air quality, including visibility [*McMeeking et al.*, 2006; *Park et al.*, 2006;
49 *Park et al.*, 2007; *Phuleria et al.*, 2005; *Robinson et al.*, 2006]. For example, *Park et al.* [2007]
50 estimated that biomass burning contributed about 50% of the annual mean total particulate
51 carbon (TC) concentrations across the continental U.S., with summer wildfires identified as the
52 most important driver of interannual variability in observed TC concentrations [*Spracklen et al.*,
53 2007]. Further, it is expected that the frequency and magnitudes of wildfires will increase in
54 coming decades in regions affecting the U.S. [*Spracklen et al.*, 2007], which, along with
55 increased demand for prescribed burning to reduce fuel loads in vulnerable regions [e.g., *Haines*
56 *et al.*, 2001], will result in increasing impacts from biomass burning.

57 Model estimates of fire emissions and their impacts require not only burned-area and fuel
58 loading inventories, but also fuel-based emission factors (EF) for both gaseous and particulate
59 phase emissions. Emission factors relate the mass of a chemical species emitted to the mass of
60 fuel burned [e.g., *Park et al.*, 2007; *Schultz et al.*, 2008; *Wiedinmyer et al.*, 2006]. EF have been
61 measured in the laboratory and in the field for at least the last 40 years, but they remain a
62 significant source of uncertainty in regional and global estimates of fire emissions [*Schultz et al.*,
63 2008; *Wiedinmyer et al.*, 2006]. Most EF measurements have concentrated on fuels from regions

outside of the continental U.S., since these account for the largest fractions of global emissions and thus have the most significant impacts on global tropospheric chemistry. *Andreae and Merlet* [2001] conducted an extensive literature review and compiled recommended EFs for three primary ecosystem types: savanna and grassland, tropical forests, and extratropical forests. These EFs have been applied in many modeling studies [e.g., *van der Werf et al.*, 2006]. Although *Andreae and Merlet* [2001] included North American fuels in their survey, the recommended average values do not necessarily reflect the specific fuel types and combustion conditions most important at U.S. local and regional scales.

*Battye and Battye* [2002] summarized much of the work reported in the peer-reviewed and grey literature that applied to emissions from U.S. wildland fires, with a focus on field studies, primarily airborne, of emissions from fires in forested regions in the northwestern US. and Alaska, as well as chaparral fires and fires in the southeastern U.S. [*Cofer et al.*, 1988a; *Cofer et al.*, 1988b; *Friedli et al.*, 2001; *Hardy et al.*, 1996; *Hays et al.*, 2002; *Muhle et al.*, 2007; *Yokelson et al.*, 1999]. While field studies have the advantage of measuring emissions from an actual fire, as pointed out by *Yokelson et al.* [2008], they offer only a snapshot in time, space, and combustion phase, and the number of measured species is limited. Controlled laboratory studies can be used to fill in some of these gaps. Some recent laboratory studies of U.S.-relevant fuels have been conducted [*Chakrabarty et al.*, 2006; *Chen et al.*, 2006; *Chen et al.*, 2007; *Hays et al.*, 2002], but we are unaware of published laboratory measurements of emissions from individual chaparral or southeastern U.S. plant species. Earlier laboratory wind-tunnel studies examining several Californian fuels were primarily focused on agricultural waste [*Jenkins et al.*, 1991; *Jenkins et al.*, 1993; *Jenkins et al.*, 1996; *Turn et al.*, 1997]. There have been a number of studies focusing on characterization of source profiles, used for source apportionment estimates,

for fuels commonly consumed by residential fireplace or wood stove burning, because of their role in urban and suburban air quality degradation [*Fine et al.*, 2001; 2002a; b; 2004; *Lipsky and Robinson*, 2006; *Roden et al.*, 2006]. Finally, very few studies have presented a comprehensive set of measurements that include both gas-phase and speciated particulate-phase emissions, along with an indicator of combustion conditions.

The Fire Laboratory at Missoula Experiment (FLAME) aimed to fill some of the gaps in available data on emissions from fires in the U.S. The study took place at the US Forest Service's Fire Sciences Laboratory (FSL) in 2006 (FLAME 1) and 2007 (FLAME 2). Earlier experiments performed at the FSL examined fire combustion behavior [*Freeborn et al.*, 2008], trace gas emissions [*Christian et al.*, 2004; *Goode et al.*, 1999; *Yokelson et al.*, 1996; *Yokelson et al.*, 1997] and aerosol emissions [*Chakrabarty et al.*, 2006; *Chen et al.*, 2006; *Chen et al.*, 2007; *Engling et al.*, 2006; *Freeborn et al.*, 2008]. FLAME expanded on this work by including additional fuels and fuel components most relevant to wildland fire and prescribed burning in the U.S., and adding/improving measurements of aerosol properties, including emissions of smoke marker species [*Sullivan et al.*, 2008], mercury compound emissions [*Obrist et al.*, 2008], particle size distributions and refractive index [*Levin et al.*, in preparation], aerosol hygroscopicity, cloud condensation nuclei (CCN) and ice nuclei (IN) activity [*Petters et al.*, 2009], and aerosol optical properties [*Lewis et al.*, 2008; *Mack et al.*, in preparation].

## 2. FUEL SELECTION AND TREATMENT

Leaves and woody material from 33 unique plant species (Table 1) were burned individually and in various combinations during FLAME 1 and 2. Fuels that were too moist to burn were dried at 35°-40° C for 48–72 hours. The remaining untreated fuels had dried sufficiently during shipping and storage to be used without drying. Fuel moisture (FM, dry

weight percent; see Table S1) for each fuel as used was determined by holding a sample at 100° C for 48 hours and measuring the mass loss. Fuel carbon and nitrogen contents (Table 1) were measured by an independent laboratory. We selected fuels based on their modeled frequency of consumption in wild- and prescribed fires in the western and southeastern United States and in fire-impacted regions in close proximity to urban areas. We further prioritized selection of species for which little or no peer-reviewed, controlled laboratory emissions data were available.

## 2.1. Chaparral

Chaparral is a highly diverse ecosystem that is distributed from Baja California to south-central Oregon and covers approximately 6% of the area of California [*Keeley and Davis*, 2007]. Chaparral-dominated regions coincide with many highly populated areas in California, most notably the Los Angeles and San Diego metropolitan regions, underscoring the need for accurate emission inventories for chaparral fuels. For example, *Clinton et al.* [2006] estimated that ~80% of the fuel consumed by a series of major wildfires in southern California during 2003 were shrubs and duffs. The dominant species within the chaparral ecosystem include chamise (*Adenostoma fasciculatum*) and species in the *Ceanothus* and *Arctostaphylos* genera [*Keeley and Davis*, 2007]. We tested three fuels representing this ecosystem: chamise, hoaryleaf ceanothus (*Ceanothus crassiofolis*), and Eastwood's manzanita (*Arctostaphylos glandulosa*). Samples were collected from the San Jacinto Mountains, about 150 km east of Los Angeles, California (see Table 1). Chaparral fire emissions have been observed from aircraft [*Cofer et al.*, 1988a; *Cofer et al.*, 1988b; *Hegg et al.*, 1987], but we are unaware of laboratory measurements that have appeared in the peer-reviewed literature.

## 2.2. Montane and subalpine forests

Montane and subalpine coniferous forests cover major portions of the Sierra Nevada and

Cascade mountain ranges [*Fites-Kaufman et al.*, 2007], inland regions of the northwestern U.S. [*Franklin*, 1988], and northern Rocky Mountains [*Peet*, 1988]. This region encompasses many federal Class I areas that are protected against visibility degradation. Species from this ecosystem tested during FLAME included: ponderosa pine (*Pinus ponderosa*), logdepole pine (*Pinus cortata*), and Douglas-fir (*Pseudotsuga menziesii*). We burned needles, woody material, combinations of needles and woody material, as well as litter (dead needles and cones from the forest floor) and duff (partly decayed litter including a portion of the uppermost layers of soil). These species were collected from several rural locations near Missoula, Montana. We also burned a mixture of unidentified grass species collected from a site near the FSL.

### 2.3. Rangeland

Sagebrush rangeland ecosystems are one of the most widespread in the intermountain west, primarily found in eastern Oregon, southern Idaho, Nevada and Utah [*West and Young*, 2000]. In addition to big sagebrush (*Artemisia tridentate*), we also burned two other woody species found from this region: Gray's rabbitbrush (*Chrysothamnus nauseosus*) and Utah juniper (*Juniperus osteosperma*). The rabbitbrush and juniper samples were collected near Salt Lake City, Utah. Sagebrush samples were collected from two other areas: an urban setting near the Salt Lake City airport and a rural setting near Missoula, Montana.

### 2.4. Southeastern coastal plain

Forest, rangeland and cropland undergo prescribed burning each year in the southeastern U.S. [*Haines et al.*, 2001], but wildfires also occur in this region. We burned several species common to the coastal plain region of the southeastern U.S., including longleaf pine (*Pinus palustris*), and understory shrubs such as saw palmetto (*Serenoa repens*), gallberry (*Ilex gllabra*), and wax myrtle (*Myrica cerifera*). During periods of prolonged drought, fire can spread to dry

156 savannah and wetland ecosystems, so we selected several representative species including titi
157 (*Cyrilla racemiflora*), sawgrass (*Cladium mariscus*), common reed (*phragmites australis*),
158 wiregrass (*Aristida beyrichiana*) and black needlerush (*Juncus roemerianus*). We also burned
159 kudzu (*Pueraria lobata*), an invasive species that is frequently the target of control efforts, which
160 include prescribed burning.

161 2.5. Boreal forests

162 Boreal forest fires are a major source of carbon to the atmosphere [*Kasischke et al.*,
163 1995], and their emissions have major impacts on the atmosphere on local and global scales
164 [e.g., *French et al.*, 2002; *O'Neill et al.*, 2002; *Pfister et al.*, 2008; *Stohl et al.*, 2006; *Trentmann*
165 *et al.*, 2006]. Emissions from boreal North America alone accounted for ~10% of annual
166 average global emissions from 1997-2004 [*van der Werf et al.*, 2006] and have been observed to
167 be transported into the U.S. [e.g., *Al-Saadi et al.*, 2005]. White spruce (*Picea glauca*) and black
168 spruce (*Picea mariana*) are ubiquitous conifer species in boreal forests and are commonly found
169 in spruce-feathermoss forests that dominate the southern boreal forest zone, which includes a
170 large portion of Alaska [*Elliot-Fisk*, 1988]. We burned spruce samples collected within ~50 km
171 of Fairbanks, Alaska. Wildfires and prescribed burns affect belowground biomass in addition to
172 shrubs and trees, so we also burned samples taken from forest floor (duff), which consists of the
173 uppermost layer of soil with live and dead feathermoss (*Pleurozium schreberi*). However, we
174 note that we did not have any samples of the underlying peat below the surface duff, which can
175 contribute substantially to total fire emissions [*Kasischke et al.*, 2005; *Yokelson et al.*, 1997].

176 2.6. Other fuels

177 We included a mixture of plants that are frequently burned in Puerto Rico, as biomass
178 burning emissions from this region, as well as from Mexico and Central America, can be

179 transported to the southeastern U.S. [*Kreidenweis et al.*, 2001]: teak (*Tectona grandis*), sea
180 hibiscus (*Hibiscus tiliaceus*), peltophorum (*Peltophorum inerme*), sacky sac bean (*Inga laurina*),
181 and fern (*Decranopteris pectinata*). Two agricultural waste products that are burned after harvest
182 were collected in Asia: rice straw (*oryza sativa)* from Taiwan and sugar cane (*saccharum*
183 *officenarum*) from the Guangdong province of China. Although outside the scope of our general
184 focus on U.S. inventories, emissions from these agricultural wastes have attracted recent interest
185 [*Christian et al.*, 2003; *Yokelson et al.*, 2008] and have been shown to affect air quality in
186 populated regions [*Viana et al.*, 2008; *Yang et al.*, 2006].

187 ## 3. EXPERIMENTAL METHOD

188 ### 3.1. Facility and burn procedure

189 The experiments were performed at the U.S. Forest Service's combustion testing facility
190 at the Fire Sciences Laboratory in Missoula, Montana, which is depicted in Figure 1 and has
191 been described previously [*Bertschi et al.*, 2003; *Christian et al.*, 2003; *Yokelson et al.*, 1996;
192 *Yokelson et al.*, 2008]. The main combustion chamber is a square room with internal dimensions
193 12.4 x 12.4 x 19.6 m high with a total volume of ~3000 $m^3$. Outside air was conditioned for
194 temperature and humidity and pumped into the chamber prior to each burn. An exhaust stack
195 located at the center of the room begins 2.1 m above the floor and extends through the chamber
196 ceiling. An inverted funnel at the bottom of the exhaust stack narrows from a 3.6 m diameter
197 opening to the 1.6 m stack diameter [*Christian et al.*, 2003]. Sampling ports that originate near
198 the center of the flow and pass through the walls of the exhaust stack are located ~16.5 m above
199 the floor, and are accessed from a measurement platform near the ceiling.

200 Two types of experiments were performed during FLAME, which we refer to as 'stack'
201 and 'chamber' burns (Table S1). During stack burns, emissions from the fuel bed, located

202 directly beneath the inverted funnel, were drawn through the exhaust stack. Instruments located
203 on the measurement platform continuously sampled through the platform sample ports. *Christian*
204 *et al.* [2004] used direct observations of gas profiles to confirm that emissions are well-mixed
205 across the stack. In contrast, the combustion room was sealed during chamber burns by closing
206 the exhaust stack. The fuel bed was placed about halfway between the exhaust stack and the
207 chamber wall and a large circulation fan operated in one corner to facilitate mixing. Continuous-
208 sampling instruments were relocated from the measurement platform to laboratories adjacent to
209 the combustion chamber, and drew samples through wall ports. Chamber burns were designed
210 primarily for optical closure experiments not reported here, as those measurements required
211 lower species concentrations and longer sampling periods (~2 hours) compared to those possible
212 during stack burns, which typically lasted from five to ten minutes.

213 The majority of samples burned during stack experiments were placed on a 46 x 61 cm
214 horizontal metal tray covered with an inert ceramic heat shield. Fuels were stacked horizontally
215 on the fuel bed to facilitate ignition, except for two large fuel mass burns (~2500 g) when fuels
216 were stacked in a cylindrical wire cage. The fuel bed was placed on a Mettler-Toledo PM34
217 balance to monitor its mass as a function of burn time. The initial fuel mass ($m_0$) and final
218 residual mass ($m_{residual}$), both listed in Table S1 for each burn, were measured with a higher
219 sensitivity PM34-K balance (Mettler-Toledo). Initial fuel masses ranged from 25 to 2500 g
220 depending on the objective of the experiment and desired emission concentrations; most were
221 between 100 and 250 g.

222 We ignited the fuel bed using several methods. During FLAME 1, dry fuels were ignited
223 using a butane pilot lighter applied briefly to the edge of the fuel bed. Fuels with high fuel
224 moistures required the application of a propane torch or heated metal coils for a significant

period of time, in some cases continuously, to maintain the fire. Both ignition methods often resulted in a propagating flame front that moved through the fuel bed and simultaneous flaming and smoldering combustion in different parts of the fuel bed. We modified the fuel bed in the FLAME 2 experiments [*Sullivan et al.*, 2008]. Fuels were placed on a lattice of heating tape that was soaked with ~15 g of ethanol, which was vaporized and ignited on heating, uniformly igniting the fuel bed. The dense duff core samples still required application of the propane torch to sustain combustion, but all other fuels were ignited effectively using this method. Table S1 provides the components of the plant or plants that were burned during each burn, the ignition method, and the fuel moisture content. We performed three replicate burns for each fuel type during FLAME 1 stack burns and two replicate stack burns during FLAME 2.

### 3.2. Real-time gas measurements

Real-time measurements of $CO_2$, CO, NO, and $NO_2$ were made at ~2 second resolution using three commercial gas analyzers, sampling through aluminum (C gas analyzers) or Teflon lines ($NO_x$ analyzer). Carbon dioxide and water vapor mixing ratios were measured by a Li-Cor Model 6262 non-dispersive infrared gas analyzer. Carbon monoxide mixing ratios were measured using a Thermo Environmental Model 48C variable-range gas filter correlation analyzer. Two sets of mixed standards ([$CO_2$] = 362 ppm, [CO] = 0.5 ppm and [$CO_2$] = 499 ppm, [CO] = 2.7 ppm) were passed through the analyzers prior to burn ignition for calibration. The mixing ratios of nitrogen oxides ($NO_X$ = NO + $NO_2$) were measured by a Thermo Environmental Model 42 chemiluminescence analyzer. We observed high (>2000 ppb) $NO_X$ concentrations that saturated the analyzer during several FLAME 2 burns and do not report those $NO_X$ data. In some of those cases the NO measurement was valid and is reported. The estimated accuracy/precision of the measurements were: Li-Cor, 1%/0.1%; TECO, 2%/1%.

### 3.3. Trace gas canister measurements

Canister samples of emissions drawn directly from the stack and chamber were analyzed for $CO_2$, CO, $CH_4$ (methane), $C_2H_4$ (ethene), $C_2H_6$ (ethane), $C_3H_6$ (propene), $C_3H_8$ (propane), three isomers of $C_4H_8$ (butene), and $C_4H_{10}$ (n-butane) gases with a Hewlett Packard model 5890 Series II gas chromatograph. Background samples were collected in several canisters throughout the day during the experiments and used to calculate the excess mixing ratios of each measured species (e.g., $\Delta CH_4 = CH_{4,\,measured} - CH_{4,\,background}$). The $CO_2$ and CO analyses use a 1 mL sample loop to inject the sample, and a 1/8" diameter x 6 foot Carbosphere (Alltech) column to separate $CO_2$, CO, and air with a helium carrier gas at a flow rate of 16 mL $min^{-1}$. After separation in the column the sample enters a nickel catalyst methanizer (375° C), which converts the $CO_2$ and CO to $CH_4$, and then a flame ionization detector (FID) at 350° C. The oven temperature program is isothermal at 100° C. The $C_1$-$C_4$ analyses are performed using a 0.25 mL sample loop, with a 0.53 mm x 30 m GS-Q (J&W Scientific) column with a helium carrier gas at 6 mL $min^{-1}$. The oven temperature program for this analysis is 30° C for 6 minutes, then increasing by 10° C $min^{-1}$ to a final temperature of 90° C for 8 minutes.

Chromatogram data were processed by Hewlett Packard ChemStation II software. A set of gas standards bracketing the sample concentrations were analyzed with each set of samples to construct a standard curve for each compound. Based on the integrated peak areas, the sample concentrations were calculated from the standard curves. Duplicate analyses were performed every sixth sample to quantify measurement precision error. National Institute of Standards and Technology (NIST) primary standards of $CO_2$, CO, and $CH_4$ were analyzed as samples to measure overall accuracy. Accuracies/uncertainties in the GC analyses are 1%/1% for $CO_2$, CO, and $CH_4$, and 10%/10% for $C_{2\text{-}4}$ gases.

271 3.4. Trace gas denuder measurements

272 We measured ammonia ($NH_3$), nitric acid ($HNO_3$), and sulfur dioxide ($SO_2$) concentrations
273 emitted from fires using annular denuders (URG Corporation, Chapel Hill, NC). The denuders
274 operated in series with a filter sampling system (see Section 3.5). The sample flow was
275 nominally 10 L $min^{-1}$ and was pulled through a Teflon-coated inlet; *Brauer et al.* [1989] cite
276 efficiencies of 97.3-98.5% for sampling of $NH_3$ through similar inlets. The $HNO_3$ denuder was
277 coated with 10 mL of a 1% sodium carbonate + 1% glycerol in a 1:1 methanol/water solution
278 and the $NH_3$ denuder was coated with 10 mL of a 1% phosphorous acid in a 9:1 methanol/water
279 solution [*Perrino et al.*, 1990; *Perrino and Gherardi*, 1999]. Coated denuders were dried with $N_2$
280 for ~10 minutes. After sampling, each denuder was extracted using 10 mL of deionized water.
281 Extracts were analyzed using a Dionex DX-500 series ion chromatograph. Details of the analysis
282 procedure are given by *Yu et al.* [2006] and *Lee et al*. [2008]. Minimum detection limits (MDL)
283 for each species were determined from blank samples and values below the MDL are not
284 reported.

285 3.5. Particulate filter samplers

286 Three types of filter samplers collected particulate matter on filters during the burns for
287 compositional analysis: a URG annular denuder/filter sampling system (URG, Chapel Hill,
288 North Carolina), a high-volume sampler (Hi-vol; Thermo Anderson, Smyrna, Georgia), and two
289 IMPROVE (Interagency Monitoring of Protected Visual Environments) samplers [*Malm et al.*,
290 2004]. The Hi-vol and URG samplers were located on the sampling platform during stack burns.
291 During chamber burns, they were moved to the chamber floor, with the Hi-vol samplers on
292 tables to keep the inlets of both samplers at a uniform height (~3 m). The IMPROVE samplers
293 had inlets at a similar height, and only ran during chamber burns because of space restrictions on

294 the stack sampling platform. During stack burns, the filter sampler pumps were turned on 30
295 seconds prior to ignition and turned off when the fire was considered extinguished based on
296 visual observations. During chamber burns, the filter sampler pumps were started approximately
297 four minutes after ignition, and individual aerosol samples for each burn were typically collected
298 over two hours.

299 The Hi-vol sampler collected sample on quartz filters for thermal optical OC/EC analysis.
300 *Sullivan et al.* [2008] and *Engling et al.* [2006] described the Hi-vol sampler we used during
301 FLAME. The sampler had a nominal flow rate of 1.13 $m^3$ $min^{-1}$. An assembly of two quartz-fiber
302 filters collected particles divided into two size classes: those with aerodynamic diameters ($D_{ae}$) >
303 2.5 μm (coarse mode) and those with $D_{ae}$ < 2.5 μm (fine mode). We only present results from the
304 analysis of the 20.3 x 25.4 cm fine mode filter—equivalent to particulate matter (PM) with $D_{ae}$ <
305 2.5 μm or $PM_{2.5}$—because an examination of the IMPROVE filters and volume size distributions
306 [*Levin et al.*, in preparation; *Sullivan et al.*, 2008] confirmed that total aerosol mass was
307 dominated by particles in the sub-2.5 μm diameter size range, as expected [e.g., *Ward and*
308 *Hardy*, 1991]. The quartz filters were wrapped in aluminum foil and baked in an oven over a 36
309 hour period (12 hour heating at 550° C + 24 hour cool down) prior to sampling to remove any
310 organic contaminants. Punches from the hi-vol filters were analyzed for the masses of carbon in
311 the OC and EC fractions with a semi-continuous analyzer (Sunset Laboratory, Tigard, Oregon)
312 in 'off-line' mode [*Sullivan and Weber*, 2006]. The OC/EC measurements reported here were the
313 average of two 1.4 $cm^2$ punches from the same filter to reduce measurement uncertainties
314 associated with sample loading heterogeneity [*Gorin et al.*, 2006].

315 The URG sampling system consisted of two annular denuders and a filter pack arranged
316 in series, which collected aerosol samples for ion chromatography (IC) analysis [*Lee et al.*,

2004]. The 10 lpm sample flow first passed through a Teflon-coated 2.5 μm size cut cyclone to remove large particles, and then through two denuders (Section 3.4) and a nylon filter (Gelman Nylasorb, 1.0 μm pore size). A backup cellulose filter coated in citric acid collected any $NH_3$ lost from the particles collected on the nylon filter. The URG filters were extracted using 6 mL of deionized water. Extracts were analyzed for inorganic species ($Cl^-$, $SO_4^{2-}$, $NO_3^-$, $Na^+$, $NH_4^+$, $K^+$, $Mg^{2+}$, and $Ca^{2+}$) using two Dionex DX-500 IC systems.

Particles were also collected by two IMPROVE sampling systems during the chamber burns, slightly modified from those used in the IMPROVE network [*Malm et al.*, 2004]. Each system had only A, B and C modules, holding Teflo, Nylasorb, and quartz filters, respectively, and collected particulate matter after $PM_{2.5}$ or $PM_{10}$ inlets. The C modules held two quartz filters in series to characterize organic aerosol sampling artifacts. During several FLAME 1 burns, the IMPROVE modules operated for different time intervals than the other samplers; in those cases smoke species concentrations were corrected using measurements of the room air background concentrations and the total time that room air was sampled. Gravimetric mass was measured from Module A filters following the standard procedure used for samples collected in the IMPROVE network, with relative humidity in the weighing laboratory maintained between 20–40%.

### 3.6. Organic and elemental carbon thermal optical analysis (TOA) protocols

The OC and EC measurements presented here were obtained using two different protocols. Samples collected by the IMPROVE sampler were analyzed using the IMPROVE_A analysis protocol [*Chow et al.*, 2007], in which the sample is heated to four temperature plateaus (140, 280, 480 and 580 °C) in pure helium and three temperature plateaus (580, 740 and 840 °C) in 98% helium and 2% oxygen. Analysis of the hi-vol punches using the Sunset analyzer

340 followed a modification of the NIOSH 5040 protocol [*Bae et al.*, 2004; *Birch and Cary*, 1996].
341 The sample punch was heated in pure helium to 600 °C in 80 seconds and then to 840 °C in 90
342 seconds. The sample was cooled for 35 seconds and oxygen added to the analysis atmosphere
343 (98% He, 2% $O_2$). Punches were then heated to 550 °C in 30 seconds, 650 °C in 45 seconds, and
344 850 °C in 90 seconds.

345 Figure 2 compares EC/TC ratios measured for the IMPROVE $PM_{2.5}$, IMPROVE $PM_{10}$,
346 and hi-vol filter samples collected during FLAME. The good agreement between EC/TC ratios
347 found for the IMPROVE $PM_{10}$ and $PM_{2.5}$ samples ($r^2$ = 0.95, regression coefficient = 0.98)
348 shows that the EC fraction of TC was similar in both. EC/TC ratios obtained by the same
349 protocol for high EC/TC ratios were strongly correlated, but they disagreed within about a factor
350 of two between protocols for samples with low EC/TC ratios, similar to the discrepancies found
351 in biomass burning-impacted samples in previous studies [*Watson et al.*, 2005]. It is unclear
352 which method provides a more accurate measure of the EC content of the aerosol. In the
353 remainder of this work, we use the Hi-vol/NIOSH 5040/Sunset OC and EC measurements,
354 simply because they are a more complete data set (available for both stack and chamber burns).

355 Filter-based carbonaceous aerosol measurements are prone to artifacts caused by gas-
356 phase adsorption onto filter fibers (positive artifact) and volatilization of the sampled particle
357 phase organic material (negative artifact) [e.g., *Kirchstetter et al.*, 2001; *Mader and Pankow*,
358 2001; *Turpin et al.*, 1994]. During FLAME, the IMPROVE $PM_{2.5}$ and IMPROVE $PM_{10}$ samplers
359 collected aerosol using front and back quartz filters arranged in series. Ideally, the mass of OC
360 (adsorbed gases) measured on the back filter equals the mass of OC measured on the front filter
361 that was due to adsorbed gases. Overall, adsorption artifacts during FLAME appeared to be
362 relatively small (Figure 3). At high OC concentrations (> 100 μg $m^{-3}$), when presumably more

semi-volatile material was in the particle phase, back filter OC was ~2–5% of the front filter OC. At lower OC concentrations (< 50 μg $m^{-3}$), when more semi-volatile material should be in the gas phase, back filter OC approached 20% of the front filter OC, closer to the 20-50% values reported by *Fine et al.* [2001] and *Lipsky and Robinson* [2005; 2006]. In those studies, the aerosol samples were diluted to lower concentrations than we sampled during FLAME, which may have altered the partitioning of semi-volatile species toward the gas phase.

### 3.7. Emitted and consumed mass calculations

For the canister and denuder measurements, the total emitted mass of each species was computed from the product of the excess mixing ratios and the sample volume. The canister and denuder samplers operated throughout each stack burn and represent fire-integrated emissions. The continuous measurements of CO and $CO_2$ during chamber burns showed that the concentrations of these species did not vary significantly after the chamber became well mixed, within 30 minutes of ignition. The canisters were used to grab a sample from the chamber approximately 60 minutes into the experiment.

During the stack burns, filter and denuder samples were collected over multiple, replicate burns to ensure adequate concentrations for compositional analysis, particularly trace organic species [*Sullivan et al.*, 2008]. We usually sampled three replicate burns on a single filter during FLAME 1 and two replicate burns on a single filter during FLAME 2. To calculate emission factors for each aerosol species, we multiplied the mass concentrations of each species determined from the filter measurements by the total volume of air sampled through the stack. We calculated the mass of aerosol species emitted during the chamber burns by multiplying mass concentrations determined from filter measurements by the total volume of the chamber. This assumes that the emissions were well mixed, and therefore the calculations of emission factors

386 for chamber burns have higher uncertainty than those for stack burns.

387 The mixing ratio measurements from the real-time gas analyzers were multiplied by the
388 volume flux of air through the stack and integrated over the lifetime of the burn to obtain the
389 total mass of CO, $CO_2$ and $NO_X$ emitted during the stack burns. For chamber burns, we
390 calculated the average gaseous-species mixing ratios for the period from 30 to 35 minutes
391 following ignition, and multiplied by the chamber volume.

392 We adjusted the total mass of CO and $CO_2$ emitted for burns that used the ethanol-coil
393 ignition system by subtracting the mean of the total emissions for each species during the two
394 ethanol-coil test burns (0.13 g CO, 12.5 g $CO_2$). In general, the mass of plant material burned
395 was 5-10 times greater than the mass of ethanol consumed during the ignition procedures.
396 Exceptions were burns featuring low fuel masses conducted during FLAME 2 chamber burns.
397 Emission data for burns that used the propane torch ignition method were adjusted by subtracting
398 the total torch emissions, which were determined by multiplying the time the torch was on by the
399 species emission rate. Burns that required the torch to be applied to maintain combustion for a
400 period greater than half of the total burn time are omitted in the analyses.

401 The mass of dry biomass consumed ($m_{\text{consumed}}$), assuming the residual material contains
402 no water, was calculated as:

$$m_{consumed} = \frac{m_{fuel}}{1 + FM} - m_{residual} \qquad 1$$

403 where $FM$ is the fuel moisture fraction, $m_{\text{fuel}}$ is the initial (wet) fuel mass and $m_{\text{residual}}$ is the mass
404 of ash and unburned fuel remaining. The carbon consumed ($C_{\text{consumed}}$) during each burn was
405 calculated by multiplying $m_{\text{consumed}}$ by $x_c$ (Section 3.9).

406 3.8. Modified combustion efficiency calculation

407 Since biomass burning emissions are known to depend on the combustion conditions, it is
408 useful to include a measure of the combustion efficiency in reporting observations. We adopt the
409 approach used in many prior studies [e.g., *Yokelson et al.*, 2008] and report the fire-integrated
410 modified combustion efficiency, MCE, which depends on the molar ratio of the emitted CO and
411 $CO_2$ [*Ward and Radke*, 1993]:

$$MCE = \frac{\Delta[CO_2]}{\Delta[CO] + \Delta[CO_2]} \quad (2)$$

412 where $\Delta[CO_2]$ and $\Delta[CO]$ are the fire-integrated excess molar mixing ratios of $CO_2$ and CO. To
413 compute the excess quantities, we assumed the ambient concentrations of CO and $CO_2$ were
414 equal to their mean values measured in the stack or chamber immediately prior to ignition
415 (usually from 120 to 10 seconds before ignition). For stack burns, we determined the fire-
416 integrated MCE for each burn by dividing the total mass of $CO_2$ (in g C) emitted by the net mass
417 of $CO_2$ plus CO emitted, also in g C. For chamber burns, we computed the mean fire-integrated
418 MCE during the 5-minute period between 30 and 35 minutes following ignition, as was done for
419 other gases (Section 3.7). Table S1 lists the fire-integrated MCE for each burn.

420 3.9 Emission ratios and emission factors

421 Fire-integrated emission factors were calculated using the carbon mass balance (CMB)
422 approach [*Ward and Radke*, 1993], in which the concentrations of emitted carbon-containing
423 species are a proxy for the mass of dry fuel consumed during the fire. The emission factor for
424 species *i* emitted by a fuel with carbon mass fraction ($x_c$) of the dry fuel mass is given by:

$$EF_i = \frac{m_i}{CO + CO_2 + PM_C + \Sigma HC} x_c \quad (3)$$

425 where $m_i$ is the mass of species *i* emitted, $PM_C$ is the mass of particulate-phase carbon and ΣHC

426 is the sum of the total mass of C contained in gas-phase hydrocarbons, estimated during FLAME
427 as the sum of the measured $C_{1\text{-}4}$ hydrocarbons. We used the measured values of dry fuel mass $x_c$
428 reported in Table 1 or assumed a value of 0.45 [*Andreae and Merlet*, 2001] in the absence of fuel
429 carbon information. To report gas-phase emission factors on a burn-by-burn basis we must
430 ignore the $PM_c$ term in Equation 3, but it is usually a small fraction of the carbon emissions
431 [*Lipsky and Robinson*, 2006] and, together with the contribution from carbon-containing gases
432 not measured, causes an overestimation of EF on the order of only 1-2% [*Andreae and Merlet,*
433 2001]. All emission factors reported here are in units of g species per kg dry fuel, unless stated
434 otherwise.

435 ## 4. RESULTS

436 ### 4.1. Fire behavior and combustion efficiency

437 Fire-integrated MCE values ranged from approximately 0.75–0.95, but we also observed
438 MCE values outside this range for burns in which we only sampled flaming or smoldering phase
439 emissions (see Table S1). Our best estimate of the variability in fire-integrated MCE for a single
440 fuel was derived from 15 replicate ponderosa pine needle litter burns with constant FM (9.9 ±
441 0.5%) and initial fuel mass (246 ± 6 g), for which we calculated fire-integrated MCE values
442 ranging from 0.88 to 0.94 with a mean and standard deviation 0.92 ± 0.02.

443 In some cases, fuels with higher FM tended to have lower fire-integrated MCE,
444 indicating smoldering combustion contributed more to emissions than did flaming combustion,
445 as might be expected (Figure 4). For example, untreated ponderosa pine needles (FM ~60%) had
446 a fire-integrated MCE of 0.86 whereas dry ponderosa pine needles (FM ~10%) had a fire-
447 integrated MCE of 0.94. However, factors other than FM affected MCE. We observed larger
448 MCE values when we increased the mass of fuel while holding fuel moisture constant during a

449 series of ponderosa pine needle burns. Burning different plant components also resulted in
450 different combustion behavior; we observed higher MCE for chamise and Douglas fir woody
451 material compared to leaves and needles.

452 4.2. Total particulate emissions

453 The gravimetric mass concentration data from the chamber burns confirmed that the
454 $PM_{10}$ mass concentrations were dominated by $PM_{2.5}$ mass concentrations (Figure 5). The $PM_{10}$ to
455 $PM_{2.5}$ mass ratio was 1.09, estimated from a zero-intercept linear regression of all but the three
456 highest-concentration samples. The ratio increased to 1.16 if all samples were included in the
457 regression. On average, aerosol emissions were dominated by carbon and TC made up almost
458 90% of reconstructed $PM_{2.5}$ mass emissions, which we computed by summing all identified
459 aerosol species, as gravimetric data were only available for chamber burns:

460 $$\text{reconstructed } PM_{2.5} = \sum(\text{ionic species})_{URG} + EC + OC \times 1.5 \qquad 4$$

461 The rationale for the factor of 1.5 is discussed in Section 4.3.4. We observed a large range in
462 fire-integrated $PM_{2.5}$ emission factors (1.9–82.1 g $kg^{-1}$ fuel). Since OC dominated $PM_{2.5}$ and its
463 emissions are higher in smoldering combustion, the $PM_{2.5}$ EF also depended on MCE. *Reid et al.*
464 [2005] estimated fine aerosol emission factors of ~9 g $kg^{-1}$ fuel based on flaming combustion
465 measurements—which they define as MCE > 0.9—and ~34 g $kg^{-1}$ fuel for smoldering
466 combustion measurements (MCE < 0.9). *Yokelson et al.* [2008] obtained an average $EFPM_{2.5}$ of
467 9.93 g $kg^{-1}$ dry fuel in their laboratory studies of tropical fuels, similar to the recommendation of
468 *Reid et al.* [2005], with variations between 2.17 and 16.61 g $kg^{-1}$ for various fuels that had fire-
469 integrated MCEs between 0.88 and 0.979. *Ward and Hardy* [1991] recommended $EFPM_{2.5}$ of 10
470 g $kg^{-1}$ for cured grasses, 15 g $kg^{-1}$ fuel for chaparral and palmetto/gallberry fires and 20-50 g $kg^{-1}$
471 for long-needled conifer fires. In FLAME, the average $EFPM_{2.5}$ for chaparral species was 11.6 ±

15.1 g $kg^{-1}$ dry fuel; for palmetto, 11.4 ± 10.5 g $kg^{-1}$ dry fuel; and for montane fuels (long-leaf conifers) 29.4 ± 25.1 g $kg^{-1}$ dry fuel, on average, all very similar to previous recommendations.

## 4.3. Carbon species

### 4.3.1. Total carbon mass balance

We calculated the mass of carbon emitted ($C_{emitted}$) during each burn by adding together carbon emitted in the form of $CO_2$, CO, $CH_4$, $C_{2-4}$ hydrocarbons, and particle-phase OC and EC, for burns where all of these measurements were available. Figure 6 compares $C_{emitted}$ to $C_{consumed}$, with the points coded by burn type and shaded by FM because the assumption of zero residual water content may not be valid for high moisture content fuels. The masses of carbon emitted and consumed were highly correlated ($r^2$ = 0.96) and close to the 1:1 line, indicating that emissions were effectively captured by the stack and could justifiably be assumed to be well-mixed in the chamber. On average, 89 ± 5.7% of the carbon was emitted in the form of $CO_2$, followed by CO (6.9 ± 3.0%), OC (2.3 ± 2.5%), $C_2$-$C_4$ hydrocarbons (1.3 ± 1.9%), $CH_4$ (0.5 ± 0.4%), and EC (0.2 ± 0.2%).

### 4.3.2. Carbon monoxide and carbon dioxide

We report fire-integrated emission factors for CO and $CO_2$ in Table S1 and emission factors averaged for each plant species and ecosystem classifications described in Section 2 in Table 2. The species and ecosystem data are the averages of all burns for that species or ecosystem type, so the numerical values depend on the number and variety of burns performed. The emission factors for many species are driven by the relative contributions from flaming and smoldering combustion during each burn, as expressed through fire-integrated MCE in this work, and the carbon abundance in the fuel. For example, Alaskan duff featured a strong contribution

494 from smoldering combustion (average MCE = 0.867 ± 0.074), but had a lower CO emission
495 factor than several fuels with higher average MCE because it contained less carbon per unit mass
496 (Table 1).

497 The average $EFCO_2$ for montane fuels was 1552 ± 150 g $kg^{-1}$ dry fuel (mean ± 1 standard
498 deviation), near the 1569 ± 131 g $CO_2$ $kg^{-1}$ dry fuel recommended by *Andreae and Merlet* [2001]
499 for extratropical forests. The $EFCO_2$ for rangeland fuels was somewhat lower (1489 ± 176 g $kg^{-1}$
500 dry fuel) and for coastal plain fuels was somewhat higher (1632 ± 150 g $kg^{-1}$), reflecting the
501 different contributions from flaming and smoldering combustion quantified through the fire-
502 integrated MCE. The average EFCO for montane fuels was 92 ± 34.1 g $kg^{-1}$ dry fuel, somewhat
503 lower than the value recommended by *Andreae and Merlet* [2001] for extratropical forests (107
504 ± 37 g $kg^{-1}$ dry fuel). Rangeland and chaparral fuels had similar average EFCO as montane fuels,
505 but the average coastal plain value was lower (78.0 ± 27.7 g $kg^{-1}$ dry fuel), again reflecting
506 different average contributions of flaming and smoldering combustion.

507 4.3.3. Gas-phase hydrocarbons

508 Fire-integrated emission factors for most of the measured hydrocarbon species were
509 positively correlated with MCE, with coefficients of variation ($r^2$) ranging from 0.39–0.67. In
510 Figure 7, we compare our results to the regressions reported by *Christian et al.* [2003] for
511 emissions from grasses and several species from the African savanna, Indonesia and North
512 American forests burned at the FSL. The FLAME and *Christian et al.* [2003] regressions for
513 $CH_4$ were in nearly perfect agreement. The two studies took place in the same facility, but
514 examined different fuels, and used a different method to determine $CH_4$ concentrations (gas
515 chromatography versus open path FTIR). *Yokelson et al.* [2003] measured slightly higher
516 emission factors for $CH_4$ over African savanna fires, but obtained a similar slope. A number of

517 FLAME samples fall on the *Yokelson et al.* [2003] regression, but it is unclear if this is just a
518 coincidence or reflects a systematic difference in $CH_4$ emissions for different fuels or fire
519 regimes. The FLAME emission factors for $C_2H_2$ and $C_2H_4$ were higher than the *Yokelson et al.*
520 [2003] and *Christian et al.* [2003] regressions predicted, but both of those studies examined a
521 narrower range of higher MCEs than those achieved in FLAME. The least-squares fitting method
522 used for the FLAME regressions was strongly influenced by the high emission factor values we
523 observed at low MCE. The regression coefficients of the previous studies represent the data in
524 Figure 7 for samples with fire-integrated MCE values above 0.85; our data suggest that modeled
525 emissions from fires with lower MCE may be underpredicted by the prior-recommended EFs.

526 4.3.4. Carbonaceous aerosols

527 Elemental carbon emissions are associated with flaming-phase combustion, consistent
528 with temperature and oxidant-dependent soot formation mechanisms. Figure 8 illustrates the
529 relationship between fire-integrated MCE and EC/TC for emissions from two fuel classes during
530 FLAME: needle and branch components of ponderosa pine (Figure 8a) and several chaparral and
531 desert shrub fuels, including sagebrush, chamise, and manzanita (Figure 8b). EC/TC ratios were
532 less than 10% for MCE values below ~0.93, and increased strongly for MCE > 0.93 for both fuel
533 classes. The EC/TC ratio was ~0 for a sample collected during only the smoldering phase of the
534 fire (MCE = 0.80) and 0.5 for a sample collected during the flaming phase (MCE = 0.99).

535 The relationships in Figure 8 were similar to previous measurements for similar fuels.
536 *Battye and Battye* [2002] summarized recommended EF derived from a number of airborne field
537 studies reported in the grey literature. For Ponderosa pine, EC/TC ratios for flaming / smoldering
538 combustion were 0.06 / 0.16; for chaparral species in smoldering combustion, 0.11, whereas
539 flaming conditions yielded 0.11-0.22. Findings from prior laboratory studies are shown in Figure

8 (*Chen et al.* [2007], *Hays et al.* [2002], *Iinuma et al*. [2007], *Christian et al.* [2003]). Note that *Hays et al.* [2002] did not report fire-integrated MCE, so we estimated fire-integrated MCE from their reported time series of $\Delta[CO_2]$ and $\Delta$[CO] mixing ratios, and *Iinuma et al.* [2007] reported only the median and not burn-integrated values of $\Delta$[CO] and $\Delta[CO_2]$. Further, different techniques were used to measure EC in the various studies. Nevertheless, at similar values of MCE, the various field and laboratory measurements are in general agreement. We note that the larger range of MCE accessed in the FLAME experiments enables a better overall picture of the variations in emissions with MCE. For example, conditions with MCE~0.95 are not frequently accessible during field studies since they are associated with the intense flaming phase of combustion, but our data show that large fractions of EC can be emitted by chaparral species under those conditions. This variability over a fire lifetime may be important in estimating the final total emissions of EC to the atmosphere.

The patterns in Figure 8 were not evident for all fuels. Several produced little or no EC when burned despite featuring a substantial flaming contribution and associated high MCE. These fuels—rice straw in particular—also produced particles with some of the highest inorganic mass fractions of total $PM_{2.5}$, so it is possible the two are linked. Inorganic salts may catalyze combustion of EC on the filter during the OC-stages of the TOA, but photoacoustic measurements of the aerosol made online during the burn showed the emissions were only weakly absorbing [*Lewis et al.*, 2008], confirming the lack of EC. In their microscopy analysis of aerosol emissions, *Hopkins et al.* [2007] identified a distinct category of fuels that featured a strong flaming phase when burned, but produced a significant concentration of inorganic salts and had optical properties inconsistent with EC.

Figure 9 shows fire-integrated emission factors for OC, EC, and TC for all tested fuels as

563 a function of fire-integrated MCE. The data are also tabulated by plant species and ecosystem in
564 Table 2 and for each burn in Tables S2-3. A factor of 1.5 was used to compute the total organic
565 carbon mass concentration, accounting for associated O, H, N, and other elements, from the
566 measured C mass concentrations attributed to OC. The 1.5 factor was within the range of OM-to-
567 OC factors of 1.4-1.8 for biomass burning aerosol recommended by *Reid et al.* [2005], and was
568 determined appropriate for FLAME data from comparisons of reconstructed total aerosol mass
569 concentrations with measured gravimetric mass concentrations [*Levin et al.*, in preparation].

570 Organic carbon emission factors were negatively correlated with MCE ($r^2$ = 0.36),
571 increasing, as expected, with increasing contributions from smoldering-phase combustion
572 (Figure 9a). Emission factors ranged from ~0.5 g C $kg^{-1}$ fuel at high MCE to ~50 g C $kg^{-1}$ fuel at
573 lower MCE values. Juniper, rabbitbrush, rhododendron and white spruce were examples of
574 plants with low OC emission factors, with emissions dominated by flaming combustion, as
575 reflected by the fire-integrated MCE. Examples of plants with high OC emission factors included
576 'leafy' fuels such as kudzu, turkey oak, sagebrush, and manzanita that had low fire-integrated
577 MCE. The coastal plain category had the highest average OC emission factor (12.4 ± 12.0 g C
578 $kg^{-1}$ fuel) and those in the chaparral category had the lowest (6.6 ± 10.1 g C $kg^{-1}$ fuel), but these
579 averages do not account for the relative abundances of particular plants in the ecosystem. The
580 range of OC emission factors reported in the literature is very large, even for single species, as
581 we would expect given the sensitivity of emissions to combustion conditions. OC emission
582 factors reported for ponderosa pine range from at least 3-30 g $kg^{-1}$ [*Hays et al.*, 2002]. *Andreae*
583 *and Merlet* [2001] suggest an OC emission factor for extratropical forest fires of 8.6-9.7 g $kg^{-1}$
584 fuel, somewhat lower than the averages for montane fuels we report in Table 2b, but higher than
585 the average for boreal species.

586 Elemental carbon emission factors during FLAME ranged from 0–8 g C $kg^{-1}$ fuel (Figure
587 9b). The significance of the relationship between EC and MCE was weaker ($r^2$ = 0.11) than that
588 between OC and MCE. Rangeland and coastal plain species tended to have higher EC emission
589 factors compared to fuels from other regions, but with considerable variability within the
590 classifications. The study-average EC emission factor for montane species was 0.4 ± 0.8 g $kg^{-1}$
591 fuel compared to the literature-average of 0.56 ± 0.19 reported by *Andreae and Merlet* [2001] for
592 extratropical forests. The lower MCE in FLAME sagebrush burns, compared to those reported in
593 *Chen et al.* [2007], led to averages of 0.63 ± 0.42 g $kg^{-1}$ fuel compared with 1.4 g $kg^{-1}$ fuel in that
594 earlier study. Several studies have reported EC emission factors for ponderosa pine [e.g., *Chen et*
595 *al.*, 2007; *Christian et al.*, 2003; *Hays et al.*, 2002], ranging from 0.4-2.6 g $kg^{-1}$, compared to
596 0.48 ± 0.83 g $kg^{-1}$ in our study. *Ward and Hardy* [1991] give a range of emission factors for
597 'graphitic carbon' of 0.46-1.18 g $kg^{-1}$ for fires burning in the Pacific northwest, a region with
598 large populations of ponderosa pine.
599 *De Gouw and Jimenez* [in press] recently compared emission ratios for organic aerosols
600 from a number of biomass burning sources, and found they range from approximately 60 to 130
601 μg $m^{-3}$ (ppm ΔCO)$^{-1}$ for primary organic aerosol. The study average for FLAME was higher, at
602 180 ± 170 μg $m^{-3}$ (ppm ΔCO)$^{-1}$, closer to organic aerosol / ΔCO ratios of 200 μg $m^{-3}$ (ppm ΔCO)$^{-}$
603 $^{1}$ in an aged urban/biomass burning plume near Mexico City reported by [*DeCarlo et al.*, 2008].
604 Recent work by [*Grieshop et al.*, 2009] showed that biomass burning emissions can be oxidized
605 and form secondary organic aerosol, leading to increases in the organic aerosol / ΔCO ratio, but
606 [*Capes et al.*, 2008] did not observe any increase over fires in Africa despite other evidence of
607 aging. The FLAME results show that high organic aerosol / ΔCO emission ratios can exist in

608 fresh biomass burning emissions with a high level of variability, making it difficult to draw
609 conclusions about the importance of primary and secondary sources of organic aerosol.

610 4.4. Nitrogen emissions

611 4.4.1. Gas-phase nitrogen

612 We compared the mass of $NH_3$ and $NO_X$ emitted to the mass of N consumed in the burn,
613 rather than to the N present in the fuel, to account for the N ash component. The $NO_x$
614 measurements for FLAME 2 were estimated using measurements of NO and the mean ratio of
615 $NO_2$:NO observed during FLAME 1 because an instrument malfunction prevented accurate
616 measurement of $NO_2$. The N consumed by the burn was assumed to be equal to the product of
617 the dry fuel N content and the dry mass consumed during the burn. Ammonia emissions
618 represented approximately 21 ± 20% and nitrogen oxides represented 27 ± 26% of the N
619 consumed, but $NO_X$ emissions were much larger during FLAME 2 compared to FLAME 1. In
620 FLAME 1, $NH_3$ and $NO_X$ accounted for ~15% of the N consumed on average, whereas in
621 FLAME 2 they represented ~75%. There was no strong difference in the average N contents for
622 the fuels we burned during each of the studies, and the mass of fuel used in each burn was
623 similar, so that fire size, as hypothesized by *Goode et al.* [1999], did not appear to be a factor. It
624 is possible that the changes in the ignition method between the two studies may be responsible
625 for the observed differences.

626 Laboratory and field measurements have shown that $NO_X$ is emitted primarily via
627 flaming combustion and $NH_3$ is emitted primarily by smoldering combustion [*Goode et al.*,
628 2000; *Lobert et al.*, 1991; *Yokelson et al.*, 1996]. However, emissions factors for individual
629 nitrogen species are not strongly correlated with MCE and instead depend primarily on fuel
630 nitrogen content [*Andreae and Merlet*, 2001; *Lobert et al.*, 1991]; *Yokelson et al.,* 2008]. To

account for the fuel N dependence, *Yokelson et al.* [1996], *Goode et al.* [1999] and *Goode et al.* [2000] compared molar ratios of $NH_3$ and $NO_x$ to MCE. They showed that a linear relationship between $NH_3/NO_x$ and MCE was consistent for fire emissions measured in the laboratory and field for a variety of fuels. Figure 10 compares the *Goode et al.* [2000] relationship between $NH_3/NO_X$ molar ratios and MCE with FLAME observations and other recently published data. The FLAME data points are shaded according to the absolute $NO_X$ mass emissions to illustrate increasing uncertainty in the molar $NH_3/NO_X$ ratios calculated for low $NO_X$ cases. A linear least-squares regression to the high-$NO_x$ data (defined as having absolute $NO_X$ emissions greater than 0.6 g equivalent NO) indicated that $NH_3$ makes up the majority of the identified N emissions below a fire-integrated MCE ~0.85. Most of the samples that deviated from the linear fit corresponded to burns with low $NO_X$ emissions and high uncertainties in the calculated $NH_3/NO_X$ molar ratios.

$NH_3/NO_X$ molar ratios during FLAME were about a factor of two lower than those reported and summarized by *Goode et al.* [2000] at similar MCE. *Goode et al.* [2000] treated all $NO_X$ emissions as NO because $NO_2$ mixing ratios were below their instrument's detection limits. The high-$NO_x$ FLAME data agreed with the *Goode et al.* [2000] fit if only $NH_3$:NO molar ratios are considered. Several other field measurements of $NH_3$ and $NO_X$ from open-path and aircraft-based Fourier Transform Infrared spectrometry (FTIR) published this decade also deviated significantly from the *Goode et al.* [2000] fit, as shown in Figure 10. An improved description of $NH_3/NO_X$ ratios in emissions may be important in estimates of global N budgets, as well as in source apportionment studies that reply on accurate profile information.

We calculated emission factors for NO, $NO_2$, and $NH_3$ following the same approach used to calculate CO, $CO_2$ and hydrocarbon emission factors (Table S1). Fire-integrated NO emission

654 factors ranged from 0.04 to 9.6 g NO $kg^{-1}$ dry fuel, with a study mean and standard deviation of
655 2.6 ± 2.4 g NO $kg^{-1}$ dry fuel. There was a large difference between the average FLAME 1 EFNO
656 (0.7 ± 0.5 g NO $kg^{-1}$) and the average FLAME 2 EFNO (3.9 ± 2.4 g NO $kg^{-1}$). This could have
657 been due to the larger number of N-rich grasses and other plants we tested during FLAME 2.
658 Average NO emission factors for species in the coastal plain and rangeland categories were
659 almost three times higher than for montane and chaparral species and $NH_3$ emission factors were
660 roughly 50% higher. The higher rangeland averages were due primarily to sagebrush, which had
661 emission factors for NO and $NH_3$ of 5.7 ± 0.7 and 4.3 ± 1.5 g $kg^{-1}$ fuel, respectively. The
662 FLAME sagebrush averages are considerably higher than the EFNO of 2.94 g $kg^{-1}$ and $EFNH_3$ of
663 0.19 g $kg^{-1}$ reported by *Yokelson et al.* [1996].

664 Nitric acid ($HNO_3$) concentrations measured using the denuder samplers were typically
665 much lower than the other N-containing gas species we measured. The study average emission
666 factor was 0.02 ± 0.03 g $HNO_3$ $kg^{-1}$ dry fuel, but the concentrations of $HNO_3$ were below the
667 MDL for most of the samples. Nitric acid emissions were less than 1% of the N emitted in the
668 form of NO.

669 4.4.2. Particulate nitrogen

670 We measured particulate-phase nitrogen in the form of $NH_4^+$, $NO_3^-$, and $NO_2^{2-}$ and found
671 that these species generally accounted for only a small fraction of the fuel nitrogen as well as a
672 small fraction of the total $PM_{2.5}$ mass. Nitrate emission factors ranged from 0.02–0.7 g $NO_3^-$ $kg^{-1}$
673 dry fuel, with a study-average value of 0.1 ± 0.1 g $kg^{-1}$ dry fuel. The observations span the range
674 previously reported in the literature [*Andreae et al.*, 1998; *Hays et al.*, 2002; *Hegg et al.*, 1987].
675 Emissions of nitrite were lower than $NO_3^-$ emissions by roughly a factor of two, with many
676 samples below the MDL. Including the particulate nitrogen species, we were able to identify

between 10–50% of the original fuel nitrogen, consistent with the findings of *Lobert et al.* [1990] and *Kuhlbusch et al.* [1991]. The remaining fuel nitrogen was likely emitted in the form of $N_2$, HCN, and nitrogen-containing organic species [*Yokelson et al.*, 2007] or remained in the ash following the burn.

## 4.5. Sulfur emissions

### 4.5.1. Sulfur dioxide

Sulfur dioxide emission factors ranged from approximately 0–1.5 g $SO_2$ $kg^{-1}$ dry fuel. *Andreae and Merlet* [2001] recommended an $SO_2$ emission factor of 1.0 g $SO_2$ $kg^{-1}$ dry fuel for extratropical forests. *Ferek et al.* [1998] observed $SO_2$ emission factors in the tropics ranging from roughly 0.2–1.5 g $SO_2$ $kg^{-1}$ C burned, which corresponds to a range of roughly 0.1–0.7 g $SO_2$ $kg^{-1}$ dry fuel assuming a fuel C fraction of 0.45. *Ferek et al.* [1998] noted that $EFSO_2$ increased weakly with MCE, but did not observe a strong correlation between MCE and $EFSO_2$, which was also not observed in our dataset.

### 4.5.2. Sulfate

Sulfate emission factors ranged from 0–1 g $SO_4^{2-}$ $kg^{-1}$ dry fuel and were weakly correlated with MCE, increasing slightly with decreasing MCE. For savanna fires in Africa, *Sinha et al.* [2003] observed sulfate emission factors on the order of 0.2 g $SO_4^{2-}$ $kg^{-1}$ dry fuel, whereas *Andreae et al.* [1998] reported 0.6 g $SO_4^{2-}$ $kg^{-1}$ dry fuel. Even higher $SO_4^{2-}$ emission factors have been measured further from the source; e.g., the airborne data of *Andreae et al.* [1998] yielded 4–10 times higher $SO_4^{2-}$ emission factors than did ground-based measurements closer to the fire. In our experiments, $SO_2$ was emitted at roughly four times the rate of $SO_4^{2-}$. If this emitted $SO_2$ is subsequently oxidized in the atmosphere to form $SO_4^{2-}$, the combined

emission factors suggest an average yield of $SO_4^{2-}$ of 0.7 ± 0.6 g $SO_4^{2-}$ $kg^{-1}$ dry fuel.

## 4.6. Other inorganic species

### 4.6.1. Chlorine

On average, chloride was the most abundant inorganic species in the aerosol during FLAME, accounting for 26 ± 16% of the soluble inorganic and 5.4 ± 7.0% of the reconstructed $PM_{2.5}$ mass concentrations. *Reid et al.* [2005] estimated $Cl^-$ made up 2–5% of $PM_{2.5}$ in fresh biomass burning emissions and *Chen et al.* [2007] found that chloride accounted for 0.1–9.6% of $PM_{2.5}$ for several of the same fuels we burned. Emissions from several southeastern fuels burned during FLAME contained high mass fractions of chloride relative to other inorganic species. For example, chloride was ~60 % of the inorganic emissions for a palmetto leaf (*Serenoa repens*) burn.

Chloride emission factors ranged from 0.0–4.7 g $kg^{-1}$ fuel (study average, 0.6 ± 0.8 g $kg^{-1}$ fuel) and were not a function of MCE (Figure 9d). Previously-reported EFCl include ~0.0–3.2 g $kg^{-1}$ fuel [*Keene et al.*, 2006]; 0.0–1.8 g $kg^{-1}$ fuel [*Christian et al.,* 2003] and 1–2 g $kg^{-1}$ fuel [*Andreae et al.,* 1998]. Several studies showed that roughly one-third of fuel chlorine was emitted in the form of particulate matter for tropical and savannah fuels [*Christian et al.*, 2003; *Keene et al.*, 2006; *Yokelson et al.*, 2008]. Although we did not measure the fuel chlorine content, chloride mass fractions of total inorganics within fuel classes were relatively constant, indicating that fuel type and chlorine content was the major driver of chloride emissions.

### 4.6.2. Potassium

Excess (non-soil and non-sea-salt) potassium has long been used as a tracer for biomass burning aerosol [*Andreae*, 1983]. It was the second-most abundant inorganic species measured

721 during FLAME, making up 4.8 ± 5.0% of reconstructed $PM_{2.5}$ mass concentrations and 24 ±
722 13% of the inorganic mass. Potassium emission factors ranged from 0.0–4.7 g $kg^{-1}$ fuel, with a
723 study average of 0.6 ± 0.8 g $kg^{-1}$ fuel (Figure 9e). *Christian et al.* [2003] reported EFK ranging
724 from 0.02–1.29 g $kg^{-1}$ for African savanna, Indonesian peat, and several wildland plant species
725 and *Andreae and Merlet* [2001] provide literature-average values ranging from 0.08–0.41 g $kg^{-1}$
726 fuel for extratropical forests. The higher values observed in FLAME were a result of the types of
727 fuels burned. In particular, rangeland plant species had large EFK, along with many coastal plain
728 fuels. Fire-integrated molar ratios of potassium to chloride and sulfate were consistent with K
729 being in the form of predominately KCl with a minor contribution from $K_2SO_4$.

730 4.6.3. Other species

731 Sodium was 2.5 ± 3.1% of speciated fine mass on average and its mass fractions were
732 relatively independent of fuel. Calcium, magnesium and nitrite made up the remainder of the
733 analyzed inorganic species in the emissions. The totals of all measured inorganic emission
734 factors were only weakly correlated with MCE ($r^2$ = 0.12) (Figure 9f), as expected since fuel
735 composition should play the largest role in emissions of inorganic aerosol species [*Christian et*
736 *al.*, 2003; *Keene et al.*, 2006].

737 5. DISCUSSION

738 The dependencies of carbonaceous and inorganic emission factors on fuel and burn
739 characteristics have implications for predictions of biomass burning impacts on climate, air
740 quality, and visibility, because these are sensitive to the chemical composition of the aerosol.
741 Estimates of smoke aerosol optical properties require accurate information regarding combustion
742 conditions in order to estimate the relative abundance of EC and OC, which to a large extent
743 determines the single scattering albedo. Emission factors for OC and $PM_{2.5}$ are stronger functions

744 of combustion conditions, compared to EF for inorganic compounds, but depend only weakly on
745 plant species. Lack of data over a broad range of MCE may result in biased estimates of fire-
746 related aerosol amounts and properties. For example, if smoldering emissions are underestimated
747 in current biomass burning inventories, then total $PM_{2.5}$ concentrations attributable to biomass
748 burning are likely to be underestimated: (1) the emission factors for $PM_{2.5}$ increase with
749 decreasing MCE; (2) emissions of carbonaceous gas species increase with decreasing MCE, and
750 it is likely that a fraction of these eventually form secondary organic aerosol; (3) as MCE
751 decreases, more N is released in the form of $NH_3$, which can readily convert to particulate-phase
752 ammonium. On-going work is examining time-resolved aerosol mass spectrometer (AMS) data
753 obtained in the FLAME 2 studies, to examine the relationships between emissions and fire phase
754 more closely.

755 There are limits to the usefulness of the MCE in capturing other effects of the fire. *Ward*
756 *and Hardy* [1991] found that emission factors for total PM increased relative to $PM_{2.5}$ emissions
757 as fire energy release rates increased. They attributed the increased PM emissions to increased
758 turbulence for the larger fire, which lofted larger-sized PM, including ash and soil material.
759 *Andreae et al.* [1998] observed increases in the $Ca^{2+}$ and $Mg^{2+}$ content of coarse mode aerosol
760 over intense savanna fires, which they also attributed to the lofting of soil material by the
761 turbulence in the fire. This lofting effect is not captured by the MCE, nor would the laboratory
762 studies reproduce these soil emissions. Proxies for combustion behavior other than MCE may
763 provide a more practical tool for linking laboratory measurements to the modeling of observed
764 fires. For example, recent laboratory work by *Ichoku et al.* [2008] showed that fire radiative
765 energy (FRE) measured by a thermal imaging system was strongly correlated with aerosol
766 emission rates. This work could be extended to examine the relationships between FRE and

767 individual gas- and particle-phase species. An advantage of FRE-based emission factors is that
768 they can be applied to satellite measurements to develop more accurate emissions inventories.

769 Source apportionment techniques attempt to separate fire-related particles from other
770 sources and to apportion the fire-related aerosols retrospectively to various fire types such as
771 wildland, prescribed, agricultural, and residential. Most apportionment studies have been
772 conducted using chemical transport models, receptor models, and hybrids of the two. While
773 chemical transport models require accurate emission inventories, a necessary component of
774 which are accurate EF, receptor-type models require appropriate tracer species to apportion
775 sampled aerosols to these various sources. The use of a subset of FLAME data—measurements
776 of aerosol OC, water-soluble potassium, and levoglucosan, a smoke marker compound—to
777 develop better source profiles for biomass burning aerosols is discussed in *Sullivan et al*. [2008].
778 The ratios of EF we report in the Supplementary Tables for various aerosol species can also be
779 applied as source emission profiles. For example, *Park et al.* [2007] examined observed TC-to-
780 nonsoil-potassium ratios across the IMPROVE network to investigate the contributions by
781 biomass burning to annual US aerosol concentrations. They estimated TC/K ratios near 10 for
782 grassland and shrub fires in the south and ratios approaching 130 for fires in the north. We found
783 similar ratios in the emissions from individual plant species from these regions, suggesting that
784 our measured TC/K ratios could be used to estimate primary fire contributions to TC from the
785 studied fuel types.

786 ## 6. CONCLUSIONS

787 We have reported fire-integrated emission factors and aerosol mass fractions for 33
788 predominantly North American wildland plant species. Many, to our knowledge, have not been
789 previously studied in laboratory open burning experiments, including the chaparral species

790 chamise, manzanita, and ceanothus, and species common to the southeastern US (common reed,
791 hickory, kudzu, needlegrass rush, rhododendron, cord grass, sawgrass, titi, and wax myrtle).
792 These species frequently burn in wildland fires and prescribed burns near urban centres, so their
793 emissions have important effects on urban air quality. We note here that the EFs reported for EC,
794 an aerosol component that plays a key role in radiative forcing, are up to a factor of two lower
795 than those that would be obtained if an alternate analysis protocol were used to analyze the
796 filters, as shown by our comparisons for a limited number of burns. The magnitude of the
797 emission factor for EC remains a significant uncertainty in estimates of the climate impacts of
798 biomass burning.

799 To assist in the interpretation of our gas- and aerosol-phase measurements, we report the
800 corresponding fire-integrated MCE. Our results are consistent with previous work that found
801 carbonaceous gas- and particle-phase emissions depend more strongly on MCE than did the
802 emissions of inorganic species, which depend most strongly on fuel type and composition [*Ward*
803 *and Hardy*, 1991]. Combustion behavior still plays a role in the form of the inorganic emissions
804 (e.g, $NO_x$ vs. $NH_3$), but the relationships between fire-integrated inorganic gas and particle
805 emission factors and fire-integrated MCE are weak. The aerosol composition data provide a basis
806 set for interpreting simultaneous measurements of aerosol optical and hygroscopic properties,
807 CCN activity, and IN activity that were conducted during FLAME.

808 The generally consistent relationships between laboratory- and field-derived EFs that we
809 found in this work support the integrated approach advocated by *Yokelson et al.* [2008] for the
810 development of more comprehensive descriptions of EFs for use in modeling. As those authors
811 point out, different ranges of MCE are accessed in laboratory, airborne and ground-based
812 sampling strategies, and capturing EF over a large measured range of MCE can be expected to

enhance the accuracy of modeled emissions estimates. They give several examples from their own work where combining sources of data led to insights on the variation of emissions with fire phase that were not obvious from measurements over a limited range of MCE. However, two caveats in combining such data are (1) the MCE and EF we measure in the laboratory are fire-integrated, whereas those measured in a field study may represent only a portion of the burn history; and (2) the emissions in a small-scale laboratory fire do not fully reflect those in a true wildfire. Nevertheless, we have shown here, as also shown by *Yokelson et al.* [2008], that EFs for specific fuels are surprisingly consistent when interpreted through the corresponding MCE. These findings suggest value in continuing controlled laboratory studies of emissions from important fuel types that have also been observed in the field, combining the observations from various platforms and approaches to develop more robust, MCE-dependent emissions estimates.

ACKNOWLEDGEMENTS

FLAME was supported by the Joint Fire Science Program under Project JFSP 05-3-1-06, which is funded by the United States Department of Agriculture, by the National Park Service (J2350-07-5181) and by the United States Department of Energy's Office of Science (BER) through the Western Regional Center of the National Institute for Climatic Change Research. Kirchstetter was also supported by the Director, Office of Science, Office of Basic Energy Sciences, of the U.S. Department of Energy under Contract No. DE-AC02-05CH11231. We thank R. Cullin, D. Day, G. Engling, and L. Mazzoleni for their assistance in collecting samples and P. Freeborn, E. Lincoln, and the FSL staff for their help during the burns. We also thank C. McDade and L. Ashbaugh for their assistance with the IMPROVE samplers and data. FLAME fuels were provided by M. Chandler, J. Chong, D. Davis, G. Engling, G. Gonzalez, S. Grace, J. Hinkley, R. Jandt, R. Moore, S. Mucci, R. Olson, K. Outcalt, J. Reardon, K. Robertson, P.

836 Spaine, and D. Weise. GRM was supported by a Graduate Research Environmental Fellowship
837 (GREF) from the United States Department of Energy's Global Change Education Program
838 (GCEP). The manuscript has benefited immensely from the comments of three anonymous
839 reviewers and we thank them for their contributions.

840 REFERENCES


841 Al-Saadi, J., J. Szykman, R. B. Pierce, C. Kittaka, D. Neil, D. A. Chu, L. Remer, L. Gumley, E.
842 Prins, L. Weinstock, C. MacDonald, R. Wayland, F. Dimmick, and J. Fishman (2005),
843 Improving national air quality forecasts with satellite aerosol observations, *Bulletin of the*
844 *American Meteorological Society*, *86*(9), 1249-+, doi:10.1175/bams-86-9-1249.

845 Andreae, M. O. (1983), Soot carbon and excess fine potassium - Long-range transport of
846 combustion-derived aerosols, *Science*, *220*(4602), 1148-1151.

847 Andreae, M. O., T. W. Andreae, H. Annegarn, J. Beer, H. Cachier, P. le Canut, W. Elbert, W.
848 Maenhaut, I. Salma, F. G. Wienhold, and T. Zenker (1998), Airborne studies of aerosol
849 emissions from savanna fires in southern Africa: 2. Aerosol chemical composition, *Journal of*
850 *Geophysical Research-Atmospheres*, *103*(D24), 32119-32128.

851 Andreae, M. O., and P. Merlet (2001), Emission of trace gases and aerosols from biomass
852 burning, *Global Biogeochemical Cycles*, *15*(4), 955-966.

853 Bae, M. S., J. J. Schauer, J. T. DeMinter, J. R. Turner, D. Smith, and R. A. Cary (2004),
854 Validation of a semi-continuous instrument for elemental carbon and organic carbon using a
855 thermal-optical method, *Atmospheric Environment*, *38*(18), 2885-2893.

856 Battye, W., and R. Battye (2002), Development of emissions inventory methods for wildland
857 fire, 91 pp, U.S. Environmental Protection Agency, Chapell Hill, NC.

858 Bertschi, I., R. J. Yokelson, D. E. Ward, R. E. Babbitt, R. A. Susott, J. G. Goode, and W. M. Hao
859 (2003), Trace gas and particle emissions from fires in large diameter and belowground biomass
860 fuels, *Journal of Geophysical Research-Atmospheres*, *108*(D13), doi:10.1029/2002JD002100.

861 Birch, M. E., and R. A. Cary (1996), Elemental carbon-based method for monitoring
862 occupational exposures to particulate diesel exhaust, *Aerosol Science and Technology*, *25*(3),
863 221-241.

864 Brauer, M., P. Koutrakis, J. M. Wolfson, and J. D. Spengler (1989), Evaluation of the gas
865 collection of an annular denuder system under simulated atmospheric conditions, *Atmospheric*
866 *Environment*, *23*(9), 1981-1986.

867 Capes, G., B. Johnson, G. McFiggans, P. I. Williams, J. Haywood, and H. Coe (2008), Aging of
868 biomass burning aerosols over West Africa: Aircraft measurements of chemical composition,
869 microphysical properties, and emission ratios, *Journal of Geophysical Research-Atmospheres*,
870 *113*(D20), doi:D00c15
871 10.1029/2008jd009845.

Chakrabarty, R. K., H. Moosmüller, M. A. Garro, W. P. Arnott, J. Walker, R. A. Susott, R. E. Babbitt, C. E. Wold, E. N. Lincoln, and W. M. Hao (2006), Emissions from the laboratory combustion of wildland fuels: Particle morphology and size, *Journal of Geophysical Research-Atmospheres*, *111*(D7), doi:10.1029/2005JD006659.

Chen, L. W. A., H. Moosmüller, W. P. Arnott, J. C. Chow, and J. G. Watson (2006), Particle emissions from laboratory combustion of wildland fuels: In situ optical and mass measurements, *Geophysical Research Letters*, *33*(4), 4, doi:10.1029/2005GL024838.

Chen, L. W. A., H. Moosmüller, W. P. Arnott, J. C. Chow, J. G. Watson, R. A. Susott, R. E. Babbitt, C. E. Wold, E. N. Lincoln, and W. M. Hao (2007), Emissions from laboratory combustion of wildland fuels: Emission factors and source profiles, *Environ. Sci. Technol.*, *41*(12), 4317-4325.

Chow, J. C., J. G. Watson, L. W. A. Chen, M. C. O. Chang, N. F. Robinson, D. Trimble, and S. Kohl (2007), The IMPROVE-A temperature protocol for thermal/optical carbon analysis: maintaining consistency with a long-term database, *Journal of the Air & Waste Management Association*, *57*(9), 1014-1023.

Christian, T. J., B. Kleiss, R. J. Yokelson, R. Holzinger, P. J. Crutzen, W. M. Hao, B. H. Saharjo, and D. E. Ward (2003), Comprehensive laboratory measurements of biomass-burning emissions: 1. Emissions from Indonesian, African, and other fuels, *Journal of Geophysical Research-Atmospheres*, *108*(D23), 4719, doi:10.1029/2003JD003704.

Christian, T. J., B. Kleiss, R. J. Yokelson, R. Holzinger, P. J. Crutzen, W. M. Hao, T. Shirai, and D. R. Blake (2004), Comprehensive laboratory measurements of biomass-burning emissions: 2. First intercomparison of open-path FTIR, PTR-MS, and GC- MS/FID/ECD, *Journal of Geophysical Research-Atmospheres*, *109*(D2), 12, doi:10.1029/JD2003JD003874.

Clinton, N. E., P. Gong, and K. Scott (2006), Quantification of pollutants emitted from very large wildland fires in Southern California, USA, *Atmospheric Environment*, *40*(20), 3686-3695.

Cofer, W. R., J. S. Levine, P. J. Riggan, D. I. Sebacher, E. L. Winstead, E. F. Shaw, J. A. Brass, and V. G. Ambrosia (1988a), Trace gas emissions from a mid-latitude prescribed chaparral fire, *Journal of Geophysical Research-Atmospheres*, *93*(D2), 1653-1658.

Cofer, W. R., J. S. Levine, D. I. Sebacher, E. L. Winstead, P. J. Riggin, J. A. Brass, and V. G. Ambrosia (1988b), Particulate-emissions from a mid-latitude prescribed chaparral fire, *Journal of Geophysical Research-Atmospheres*, *93*(D5), 5207-5212.

Crutzen, P. J., and M. O. Andreae (1990), Biomass burning in the tropics - Impact on atmospheric chemistry and biogeochemical cycles, *Science*, *250*(4988), 1669-1678.

de Gouw, J., and J. L. Jimenez (in press), Organic aerosols in the earth's atmosphere, *Environ. Sci. Technol.*

DeCarlo, P. F., E. J. Dunlea, J. R. Kimmel, A. C. Aiken, D. Sueper, J. Crounse, P. O. Wennberg, L. Emmons, Y. Shinozuka, A. Clarke, J. Zhou, J. Tomlinson, D. R. Collins, D. Knapp, A. J. Weinheimer, D. D. Montzka, T. Campos, and J. L. Jimenez (2008), Fast airborne aerosol size and chemistry measurements above Mexico City and Central Mexico during the MILAGRO campaign, *Atmospheric Chemistry and Physics*, *8*(14), 4027-4048.

Elliot-Fisk, D. L. (1988), The boreal forest, in *North American terrestrial vegetation*, edited by M. G. Barbour and W. D. Billings, pp. 33-62, Cambridge University Press, Cambridge.

Engling, G., P. Herckes, S. M. Kreidenweis, W. C. Malm, and J. L. Collett (2006), Composition of the fine organic aerosol in Yosemite National Park during the 2002 Yosemite Aerosol Characterization Study, *Atmospheric Environment*, *40*(16), 2959-2972.

Fine, P. M., G. R. Cass, and B. R. T. Simoneit (2001), Chemical characterization of fine particle emissions from fireplace combustion of woods grown in the northeastern United States, *Environ. Sci. Technol.*, *35*(13), 2665-2675.

Fine, P. M., G. R. Cass, and B. R. T. Simoneit (2002a), Chemical characterization of fine particle emissions from the fireplace combustion of woods grown in the southern United States, *Environ. Sci. Technol.*, *36*(7), 1442-1451.

Fine, P. M., G. R. Cass, and B. R. T. Simoneit (2002b), Organic compounds in biomass smoke from residential wood combustion: Emissions characterization at a continental scale, *Journal of Geophysical Research-Atmospheres*, *107*(D21), 9, doi:10.1029/2001JD000661.

Fine, P. M., G. R. Cass, and B. R. T. Simoneit (2004), Chemical characterization of fine particle emissions from the fireplace combustion of wood types grown in the Midwestern and Western United States, *Environmental Engineering Science*, *21*(3), 387-409.

Fites-Kaufman, J. A., P. Rundel, N. Stephenson, and D. A. Weixelman (2007), Montane and subalpine vegetation in the Sierra Nevada and Cascade ranges, in *Terrestrial vegetation of California*, edited by M. G. Barbour, et al., pp. 456-501, University of California Press, Los Angeles.

Franklin, J. F. (1988), Pacific northwest forests, in *North American terrestrial vegetation*, edited by M. G. Barbour and W. D. Billings, pp. 103-130, Cambridge University Press, Cambridge.

Freeborn, P. H., M. J. Wooster, W. M. Hao, C. A. Ryan, B. L. Nordgren, S. P. Baker, and C. Ichoku (2008), Relationships between energy release, fuel mass loss, and trace gas and aerosol

emissions during laboratory biomass fires, *Journal of Geophysical Research-Atmospheres*, *113*(D1), D01301, doi:10.1029/2007JD008679.

French, N. H. F., E. S. Kasischke, and D. G. Williams (2002), Variability in the emission of carbon-based trace gases from wildfire in the Alaskan boreal forest, *Journal of Geophysical Research-Atmospheres*, *108*(D1), doi:10.1029/2001JD000480.

Friedli, H. R., E. Atlas, V. R. Stroud, L. Giovanni, T. Campos, and L. F. Radke (2001), Volatile organic trace gases emitted from North American wildfires, *Global Biogeochemical Cycles*, *15*(2), 435-452.

Goode, J. G., R. J. Yokelson, R. A. Susott, and D. E. Ward (1999), Trace gas emissions from laboratory biomass fires measured by open-path Fourier transform infrared spectroscopy: Fires in grass and surface fuels, *Journal of Geophysical Research-Atmospheres*, *104*(D17), 21237-21245.

Goode, J. G., R. J. Yokelson, D. E. Ward, R. A. Susott, R. E. Babbitt, M. A. Davies, and W. M. Hao (2000), Measurements of excess O-3, CO2, CO, CH4, C2H4, C2H2, HCN, NO, NH3, HCOOH, CH3COOH, HCHO, and CH3OH in 1997 Alaskan biomass burning plumes by airborne fourier transform infrared spectroscopy (AFTIR), *Journal of Geophysical Research-Atmospheres*, *105*(D17), 22147-22166.

Gorin, C. A., J. L. Collett, and P. Herckes (2006), Wood smoke contribution to winter aerosol in Fresno, CA, *Journal of the Air & Waste Management Association*, *56*(11), 1584-1590.

Grieshop, A. P., J. M. Logue, N. M. Donahue, and A. L. Robinson (2009), Laboratory investigation of photochemical oxidation of organic aerosol from wood fires 1: measurement and simulation of organic aerosol evolution, *Atmospheric Chemistry and Physics*, *9*(4), 1263-1277.

Haines, T. K., R. L. Busby, and D. A. Cleaves (2001), Prescribed burning in the south: trends, purpose, and barriers, *Southern Journal of Applied Forestry*, *25*(4), 149-153.

Hardy, C. C., S. G. Conard, J. C. Regelbrugge, and D. R. Teesdale (1996), Smoke emissions from prescribed burning of southern California chaparral, *Usda Forest Service Pacific Northwest Research Station Research Paper*(486), 1-&.

Hays, M. D., C. D. Geron, K. J. Linna, N. D. Smith, and J. J. Schauer (2002), Speciation of gas-phase and fine particle emissions from burning of foliar fuels, *Environ. Sci. Technol.*, *36*(11), 2281-2295.

Hegg, D. A., L. F. Radke, P. V. Hobbs, C. A. Brock, and P. J. Riggan (1987), Nitrogen and sulfur emissions from the burning of forest products near large urban areas, *Journal of Geophysical Research-Atmospheres*, *92*(D12), 14701-14709.

970 Hopkins, R. J., K. Lewis, Y. Desyaterik, Z. Wang, A. V. Tivanski, W. P. Arnott, A. Laskin, and
971 M. K. Gilles (2007), Correlations between optical, chemical and physical properties of biomass
972 burn aerosols, *Geophysical Research Letters*, *34*(18), doi:10.1029/2007GL030502.

973 Ichoku, C., J. V. Martins, Y. J. Kaufman, M. J. Wooster, P. H. Freeborn, W. M. Hao, S. Baker,
974 C. A. Ryan, and B. L. Nordgren (2008), Laboratory investigation of fire radiative energy and
975 smoke aerosol emissions, *Journal of Geophysical Research-Atmospheres*, *113*(D14),
976 doi:10.1029/2007JD009659.

977 Iinuma, Y., E. Bruggemann, T. Gnauk, K. Muller, M. O. Andreae, G. Helas, R. Parmar, and H.
978 Herrmann (2007), Source characterization of biomass burning particles: The combustion of
979 selected European conifers, African hardwood, savanna grass, and German and Indonesian peat,
980 *Journal of Geophysical Research-Atmospheres*, *112*(D8), 26, doi:10.1029/2006JD007120.

981 Jenkins, B. M., S. Q. Turn, R. B. Williams, D. P. Y. Chang, O. G. Raabe, J. Paskind, and S.
982 Teague (1991), Quantitative assessment of gaseous and condensed phase emissions from open
983 burning of biomass in a combustion wind-tunnel, *Global Biomass Burning*, 305-317.

984 Jenkins, B. M., I. M. Kennedy, S. Q. Turn, R. B. Williams, S. G. Hall, S. V. Teague, D. P. Y.
985 Chang, and O. G. Raabe (1993), Wind-tunnel modeling of atmospheric emissions from
986 agricultural burning - Influence of operating configuration on flame structure and particle-
987 emission factor for a spreading-type fire, *Environ. Sci. Technol.*, *27*(9), 1763-1775.

988 Jenkins, B. M., A. D. Jones, S. Q. Turn, and R. B. Williams (1996), Emission factors for
989 polycyclic aromatic hydrocarbons from biomass burning, *Environ. Sci. Technol.*, *30*(8), 2462-
990 2469.

991 Kasischke, E. S., N. L. Christensen, and B. J. Stocks (1995), Fire, global warming, and the
992 carbon balance of boreal forests, *Ecological Applications*, *5*(2), 437-451.

993 Kasischke, E. S., E. J. Hyer, P. C. Novelli, L. P. Bruhwiler, N. H. F. French, A. I. Sukhinin, J. H.
994 Hewson, and B. J. Stocks (2005), Influences of boreal fire emissions on Northern Hemisphere
995 atmospheric carbon and carbon monoxide, *Global Biogeochemical Cycles*, *19*(1),
996 doi:10.1029/2004gb002300.

997 Keeley, J. E., and F. W. Davis (2007), Chaparral, in *Terrestrial vegetation of California*, edited
998 by M. G. Barbour, et al., pp. 339-366, University of California Press, Los Angeles.

999 Keene, W. C., R. M. Lobert, P. J. Crutzen, J. R. Maben, D. H. Scharffe, T. Landmann, C. Hely,
1000 and C. Brain (2006), Emissions of major gaseous and particulate species during experimental
1001 burns of southern African biomass, *Journal of Geophysical Research-Atmospheres*, *111*(D4),
1002 doi:10.1029/2005JD006319.

1003 Kirchstetter, T. W., C. E. Corrigan, and T. Novakov (2001), Laboratory and field investigation of
1004 the adsorption of gaseous organic compounds onto quartz filters, *Atmospheric Environment*,
1005 *35*(9), 1663-1671.

1006 Kreidenweis, S. M., L. A. Remer, R. Bruintjes, and O. Dubovik (2001), Smoke aerosol from
1007 biomass burning in Mexico: Hygroscopic smoke optical model, *Journal of Geophysical*
1008 *Research-Atmospheres*, *106*(D5), 4831-4844.

1009 Kuhlbusch, T. A., J. M. Lobert, P. J. Crutzen, and P. Warneck (1991), Molecular nitrogen
1010 emissions from denitrification during biomass burning, *Nature*, *351*(6322), 135-137.

1011 Lee, T., S. M. Kreidenwels, and J. L. Collett (2004), Aerosol ion characteristics during the Big
1012 Bend Regional Aerosol and Visibility Observational Study, *Journal of the Air & Waste*
1013 *Management Association*, *54*(5), 585-592.

1014 Lee, T., X. Y. Yu, B. Ayres, S. M. Kreidenweis, W. C. Malm, and J. L. Collett (2008),
1015 Observations of fine and coarse particle nitrate at several rural locations in the United States,
1016 *Atmospheric Environment*, *42*(11), 2720-2732, doi:10.1016/j.atmosenv.2007.05.016.

1017 Levin, E. J. T., S. M. Kreidenweis, G. R. McMeeking, C. M. Carrico, J. J. L. Collett, W. C.
1018 Malm, and W. M. Hao (in preparation), FLAME refractive index and size distribution paper.

1019 Lewis, K., W. P. Arnott, H. Moosmüller, and C. E. Wold (2008), Strong spectral variation of
1020 biomass smoke light absorption and single scattering albedo observed with a novel dual
1021 wavelength photoacoustic instrument, *Journal of Geophysical Research-Atmospheres*,
1022 doi:10.1029/2007JD009699.

1023 Lipsky, E. M., and A. L. Robinson (2006), Effects of dilution on fine particle mass and
1024 partitioning of semivolatile organics in diesel exhaust and wood smoke, *Environ. Sci. Technol.*,
1025 *40*(1), 155-162.

1026 Lobert, J. M., D. H. Scharffe, W. M. Hao, and P. J. Crutzen (1990), Importance of biomass
1027 burning in the atmospheric budgets of nitrogen-containing gases, *Nature*, *346*(6284), 552-554.

1028 Lobert, J. M., D. H. Scharffe, W. M. Hao, T. A. Kuhlbusch, R. Seuwen, P. Warneck, and P. J.
1029 Crutzen (1991), Experimental evaluation of biomass burning emissions: Nitrogen and carbon
1030 containing compounds, in *Global Biomass Burning: Atmospheric, Climatic, and Biospheric*
1031 *Implications*, edited by J. S. Levine, pp. 289-304, MIT Press, Cambridge.

1032 Mack, L., S. M. Kreidenweis, H. Moosmüller, J. L. Collett, C. M. Carrico, W. C. Malm, W. M.
1033 Hao, and C. E. Wold (in preparation), Optical properties of aerosols during FLAME.

1034 Mader, B. T., and J. F. Pankow (2001), Gas/solid partitioning of semivolatile organic compounds
1035 (SOCs) to air filters. 3. An analysis of gas adsorption artifacts in measurements of atmospheric
1036 SOCs and organic carbon (OC) when using Teflon membrane filters and quartz fiber filters,
1037 *Environ. Sci. Technol.*, *35*(17), 3422-3432.

1038 Malm, W. C., B. A. Schichtel, M. L. Pitchford, L. L. Ashbaugh, and R. A. Eldred (2004), Spatial
1039 and monthly trends in speciated fine particle concentration in the United States, *Journal of*
1040 *Geophysical Research-Atmospheres*, *109*(D3), 33, doi:10.1029/2003JD003739.

1041 McMeeking, G. R., S. M. Kreidenweis, M. Lunden, J. Carrillo, C. M. Carrico, T. Lee, P.
1042 Herckes, G. Engling, D. E. Day, J. Hand, N. Brown, W. C. Malm, and J. L. Collett (2006),
1043 Smoke-impacted regional haze in California during the summer of 2002, *Agricultural and Forest*
1044 *Meteorology*, *137*(1-2), 25-42.

1045 Muhle, J., T. J. Lueker, Y. Su, B. R. Miller, K. A. Prather, and R. F. Weiss (2007), Trace gas and
1046 particulate emissions from the 2003 southern California wildfires, *Journal of Geophysical*
1047 *Research-Atmospheres*, *112*(D3), D03307, doi:10.1029/2006JD007350.

1048 Naeher, L. P., M. Brauer, M. Lipsett, J. T. Zelikoff, C. D. Simpson, J. Q. Koenig, and K. R.
1049 Smith (2007), Woodsmoke health effects: A review, *Inhalation Toxicology*, *19*(1), 67-106.

1050 O'Neill, N. T., T. F. Eck, B. N. Holben, A. Smirnov, A. Royer, and Z. Li (2002), Optical
1051 properties of boreal forest fire smoke derived from Sun photometry, *Journal of Geophysical*
1052 *Research-Atmospheres*, *107*(D11), doi:10.1029/2001JD000877.

1053 Obrist, D., H. Moosmüller, R. Schurmann, L. W. A. Chen, and S. M. Kreidenweis (2008),
1054 Particulate-phase and gaseous elemental mercury emissions during biomass combustion:
1055 Controlling factors and correlation with particulate matter emissions, *Environ. Sci. Technol.*,
1056 *42*(3), 721-727.

1057 Park, R. J., D. J. Jacob, N. Kumar, and R. M. Yantosca (2006), Regional visibility statistics in
1058 the United States: Natural and transboundary pollution influences, and implications for the
1059 Regional Haze Rule, *Atmospheric Environment*, *40*(28), 5405-5423,
1060 doi:10.1016/j.atmosenv.2006.04.059.

1061 Park, R. J., D. J. Jacob, and J. A. Logan (2007), Fire and biofuel contributions to annual mean
1062 aerosol mass concentrations in the United States, *Atmospheric Environment*, *41*, 7389-7400.

1063 Peet, R. K. (1988), Forests of the Rocky Mountains, in *North American terrestrial vegetation*,
1064 edited by M. G. Barbour and W. D. Billings, pp. 63-101, Cambridge University Press,
1065 Cambridge.

1066 Perrino, C., F. Desantis, and A. Febo (1990), Criteria for the choice of a denuder sampling
1067 technique devoted to the measurement of atmospheric nitrous and nitric-acids, *Atmospheric*
1068 *Environment Part a-General Topics*, *24*(3), 617-626.

1069 Perrino, C., and M. Gherardi (1999), Optimization of the coating layer for the measurement of
1070 ammonia by diffusion denuders, *Atmospheric Environment*, *33*(28), 4579-4587.

1071 Petters, M. D., M. T. Parsons, A. J. Prenni, P. J. DeMott, S. M. Kreidenweis, C. M. Carrico, A.
1072 P. Sullivan, G. R. McMeeking, E. J. T. Levin, C. E. Wold, J. J. L. Collett, and H. Moomuller
1073 (2009), Ice nuclei emissions from biomass burning, *Journal of Geophysical Research-*
1074 *Atmospheres*, *114*, D07209, doi:10.1029/2008JD011532.

1075 Pfister, G. G., P. G. Hess, L. K. Emmons, P. J. Rasch, and F. M. Vitt (2008), Impact of the
1076 summer 2004 Alaska fires on top of the atmosphere clear-sky radiation fluxes, *Journal of*
1077 *Geophysical Research-Atmospheres*, *113*(D2), doi:10.1029/2007JD008797.

1078 Phuleria, H. C., P. M. Fine, Y. F. Zhu, and C. Sioutas (2005), Air quality impacts of the October
1079 2003 Southern California wildfires, *Journal of Geophysical Research-Atmospheres*, *110*(D7),
1080 doi:10.1029/2004JD004626.

1081 Reid, J. S., R. Koppmann, T. F. Eck, and D. P. Eleuterio (2005), A review of biomass burning
1082 emissions part II: intensive physical properties of biomass burning particles, *Atmospheric*
1083 *Chemistry and Physics*, *5*, 799-825.

1084 Robinson, A. L., R. Subramanian, N. M. Donahue, A. Bernardo-Bricker, and W. F. Rogge
1085 (2006), Source apportionment of molecular markers and organic aerosol. 2. Biomass smoke,
1086 *Environ. Sci. Technol.*, *40*(24), 7811-7819, doi:10.1021/es060782h.

1087 Roden, C. A., T. C. Bond, S. Conway, A. Benjamin, and O. Pinel (2006), Emission factors and
1088 real-time optical properties of particles emitted from traditional wood burning cookstoves,
1089 *Environ. Sci. Technol.*, *40*(21), 6750-6757.

1090 Schultz, M. G., A. Heil, J. J. Hoelzemann, A. Spessa, K. Thonicke, J. G. Goldammer, A. C.
1091 Held, J. M. C. Pereira, and M. van het Bolscher (2008), Global wildland fire emissions from
1092 1960 to 2000, *Global Biogeochemical Cycles*, *22*(2), doi:10.1029/2007gb003031.

1093 Spracklen, D. V., J. A. Logan, L. J. Mickley, R. J. Park, R. Yevich, A. L. Westerling, and D. A.
1094 Jaffe (2007), Wildfires drive interannual variability of organic carbon aerosol in the western U.S.
1095 in summer, *Geophysical Research Letters*, *34*, L16816, doi:10.1029/2007GL030037.

1096 Stohl, A., E. Andrews, J. F. Burkhart, C. Forster, A. Herber, S. W. Hoch, D. Kowal, C. Lunder,
1097 T. Mefford, J. A. Ogren, S. Sharma, N. Spichtinger, K. Stebel, R. Stone, J. Strom, K. Torseth, C.
1098 Wehrli, and K. E. Yttri (2006), Pan-Arctic enhancements of light absorbing aerosol

concentrations due to North American boreal forest fires during summer 2004, *Journal of Geophysical Research-Atmospheres*, *111*(D22), doi:10.1029/2006JD007216.

Sullivan, A. P., and R. J. Weber (2006), Chemical characterization of the ambient organic aerosol soluble in water: 2. Isolation of acid, neutral, and basic fractions by modified size-exclusion chromatography, *Journal of Geophysical Research-Atmospheres*, *111*(D5), doi:10.1029/2005JD006486.

Sullivan, A. P., A. S. Holden, L. A. Patterson, G. R. McMeeking, S. M. Kreidenweis, W. C. Malm, W. M. Hao, C. E. Wold, and J. L. Collett, Jr. (2008), A method for smoke marker measurements and its potential application for determining the contribution of biomass burning from wildfires and prescribed fires to ambient PM2.5 organic carbon, *Journal of Geophysical Research-Atmospheres*, *113*, D22302, doi:10.1029/2008JD010216.

Trentmann, J., G. Luderer, T. Winterrath, M. D. Fromm, R. Servranckx, C. Textor, M. Herzog, H. F. Graf, and M. O. Andreae (2006), Modeling of biomass smoke injection into the lower stratosphere by a large forest fire (Part I): reference simulation, *Atmospheric Chemistry and Physics*, *6*, 5247-5260.

Turn, S. Q., B. M. Jenkins, J. C. Chow, L. C. Pritchett, D. Campbell, T. Cahill, and S. A. Whalen (1997), Elemental characterization of particulate matter emitted from biomass burning: Wind tunnel derived source profiles for herbaceous and wood fuels, *Journal of Geophysical Research-Atmospheres*, *102*(D3), 3683-3699.

Turpin, B. J., J. J. Huntzicker, and S. V. Hering (1994), Investigation of organic aerosol sampling artifacts in the Los Angeles basin, *Atmospheric Environment*, *28*(19), 3061-3071.

van der Werf, G. R., J. T. Randerson, L. Giglio, G. J. Collatz, P. S. Kasibhatla, and A. F. Arellano (2006), Interannual variability in global biomass burning emissions from 1997 to 2004, *Atmospheric Chemistry and Physics*, *6*, 3423-3441.

Viana, M., J. M. Lopez, X. Querol, A. Alastuey, D. Garcia-Gacio, G. Blanco-Heras, P. Lopez-Mahia, M. Pineiro-Iglesias, M. Sanz, F. Sanz, X. Chi, and W. Maenhaut (2008), Tracers and impact of open burning of rice straw residues on PM in Eastern Spain, *Atmospheric Environment*, *42*(8), 1941-1957, doi:10.1016/j.atmosenv.2007.11.012.

Ward, D. E., and C. C. Hardy (1991), Smoke emissions from wildland fires, *Environment International*, *17*(2-3), 117-134.

Ward, D. E., and L. F. Radke (1993), Emission measurements from vegetation fires: a comparative evaluation of methods and results, in *Fire in the environment: the ecological, atmospheric, and climatic importance of vegetation fires*, edited by P. J. Crutzen and Goldammer, pp. 53-76, Wiley, Chichester, UK.

1133 Watson, J. G. (2002), Visibility: Science and regulation, *Journal of the Air & Waste*
1134 *Management Association*, *52*(6), 628-713.

1135 Watson, J. G., J. C. Chow, and L.-W. Antony Chen (2005), Summary of organic and
1136 elemental/black carbon analysis methods and intercomparisons, *Aerosol and Air Quality*
1137 *Research*, *5*(1), 65-102.

1138 West, N. E., and J. A. Young (2000), Intermountain valleys and lower mountain slopes, in *North*
1139 *American terrestrial vegetation*, edited by M. G. Barbour, Cambridge University Press,
1140 Cambridge.

1141 Wiedinmyer, C., B. Quayle, C. Geron, A. Belote, D. McKenzie, X. Y. Zhang, S. O'Neill, and K.
1142 K. Wynne (2006), Estimating emissions from fires in North America for air quality modeling,
1143 *Atmospheric Environment*, *40*(19), 3419-3432.

1144 Yang, H. H., C. H. Tsai, M. R. Chao, Y. L. Su, and S. M. Chien (2006), Source identification
1145 and size distribution of atmospheric polycyclic aromatic hydrocarbons during rice straw burning
1146 period, *Atmospheric Environment*, *40*(7), 1266-1274.

1147 Yokelson, R. J., D. W. T. Griffith, and D. E. Ward (1996), Open-path Fourier transform infrared
1148 studies of large-scale laboratory biomass fires, *Journal of Geophysical Research-Atmospheres*,
1149 *101*(D15), 21067-21080.

1150 Yokelson, R. J., R. Susott, D. E. Ward, J. Reardon, and D. W. T. Griffith (1997), Emissions from
1151 smoldering combustion of biomass measured by open-path Fourier transform infrared
1152 spectroscopy, *Journal of Geophysical Research-Atmospheres*, *102*(D15), 18865-18877.

1153 Yokelson, R. J., J. G. Goode, D. E. Ward, R. A. Susott, R. E. Babbitt, D. D. Wade, I. Bertschi, D.
1154 W. T. Griffith, and W. M. Hao (1999), Emissions of formaldehyde, acetic acid, methanol, and
1155 other trace gases from biomass fires in North Carolina measured by airborne Fourier transform
1156 infrared spectroscopy, *Journal of Geophysical Research-Atmospheres*, *104*(D23), 30109-30125.

1157 Yokelson, R. J., T. Karl, P. Artaxo, D. R. Blake, T. J. Christian, D. W. T. Griffith, A. Guenther,
1158 and W. M. Hao (2007), The Tropical Forest and Fire Emissions Experiment: overview and
1159 airborne fire emission factor measurements, *Atmospheric Chemistry and Physics*, *7*(19), 5175-
1160 5196.

1161 Yokelson, R. J., T. J. Christian, T. G. Karl, and A. Guenther (2008), The tropical forest and fire
1162 emissions experiment: laboratory fire measurements and synthesis of campaign data,
1163 *Atmospheric Chemistry and Physics Discussions*, *8*, 4221-4266.

1164 Yu, X. Y., T. Lee, B. Ayres, S. M. Kreidenweis, W. Malm, and J. L. Collett (2006), Loss of fine
1165 particle ammonium from denuded nylon filters, *Atmospheric Environment*, *40*(25), 4797-4807.

1166
1167

1168

1169 TABLES

1170 Table 1. Plant species that served as fuels during FLAME.

| Common name | Scientific name | Sampling location(s) | Carbon content (%) | Nitrogen content (%) |
|---|---|---|---|---|
| Alaskan duff | - | Tok, Alaska | 31 | 0.5 |
| black spruce | *Picea mariana* | Fairbanks, AK | 55 | 0.6 |
| chamise | *Adenstoma fasciculatum* | San Jacinto Mountain, CA | 49 | 1.0 |
| common reed | *Phragmites australis* | Cameron Prairie NWR, LA | 49 | 0.5 |
| Douglas fir | *Pseudotsuga menziesii* | Missoula, MT | 54 | 0.5–0.9 |
| gallberry | *Ilex coriacea*<br>*Ilex glabra* | Sandhill Crane NWR, MI<br>St. Marks NWR, FL<br>Osceola National Forest, FL | 56 | 0.8 |
| grass | *various species* | Missoula, MT | 42 | 3.0 |
| Gray's rabbitbrush | *Ericameria nauseosa* | UT | 46 | 1.1 |
| hickory | *Carya nutt* | Hillsborough, NC | 48 | 2.1 |
| hoaryleaf ceanothus | *Ceanothus crassifolius* | San Jacinto, CA | 48 | 1.3 |
| kudzu | *Pueraria Montana* | Athens, GA | 47 | 3.6 |
| lodgepole pine | *Pinus contorta* | Missoula, MT | 42–50 | 0.3–1.2 |
| longleaf pine | *Pinus palustris* | North Carolina, Sandhill Crane NWR, MI<br>St. Marks NWR, FL<br>Camp Lejeune, NC | 52 | 1.1 |
| manzanita | *Arctostaphylos glandulosa* | San Jacinto, CA | 48 | 0.8 |
| needlegrass rush | *Juncus roemerianus* | St. Marks NWR, FL | 49 | 1.1 |
| palmetto | *Serenoa repens* | St. Marks NWR, FL<br>Osceola NF, FL<br>Sandhill Crane NWR, MS | 51 | 1.0 |
| peltophorum | *Peltophorum inerme* | Puerto Rico | 48 | 0.8 |
| ponderosa pine | *Pinus ponderosa* | Missoula, MT | 46–49 | 0.04–1.3 |
| Puerto Rican fern | *Dicranopteris pecitinata* | Puerto Rico | 46 | 0.4 |
| rhododendron | *Rhododendron minus* | - | 51 | 0.6 |
| rice straw | *Oryza sativa* | Douliou City, Taiwan | 39–46 | 0.6–0.9 |
| sagebrush | *Artemisia tridentate* | Salt Lake City, UT<br>Missoula, MT | 47–51 | 1.5–2.1 |
| sea hibiscus | *Hibiscus tiliaceus* | Puerto Rico | - | - |
| Smooth cord grass | *Spartina alterniflora* | St. Marks NWR, FL | | |
| sugar cane | *Saccharum officenarum* | Guangdon Province, China | 48 | 1.3 |
| Swamp sawgrass | *Cladium mariscus* | Big Branch Marsh NWR, LA | 48 | 2.1 |
| teak | *Tectona grandis* | Puerto Rico | 44 | 0.8 |
| titi | *Cyrilla racemiflora* | St. Marks NWR, FL | 54 | 0.9 |
| turkey oak | *Quercus laevis Walt.* | Hillsborough, NC<br>Camp Lejune, NC | 53 | 1.3 |
| Utah juniper | *Juniperus osteosperma* | UT | 49 | 0.9 |
| wax myrtle | *Myrica cerifera* | Sandhill Crane NWR, FL<br>St. Marks NWR, FL | 48–53 | 1.1–1.4 |
| white spruce | *Picea glauca* | Fairbanks, AK | 52 | 0.8 |
| wiregrass | *Aristida beyrichiana* | Sandhill Crane NWR, MS<br>St. Marks NWR, FL<br>Camp Lejeune, NC | 48 | 0.5 |

1171 Table 2a. Gas-phase emission factors for individual species and ecosystem groups. Emission
1172 factors are reported in g species $kg^{-1}$ dry fuel.
1173

| Species/Group | MCE | $CO_2$ | CO | $CH_4$ | $C_2H_4$ | $C_3H_6$ | NO | $NO_2$ | $NH_3$ | $SO_2$ |
|---|---|---|---|---|---|---|---|---|---|---|
| **Montane** | **0.915 ± 0.033** | **1552 ± 150** | **92.0 ± 34.1** | **3.7 ± 2.7** | **5.7 ± 4.8** | **1.7 ± 1.2** | **1.5 ± 1.9** | **0.7 ± 0.9** | **1.7 ± 1.4** | **0.4 ± 0.2** |
| Douglas fir | 0.906 ± 0.036 | 1579 ± 193 | 106.8 ± 32.4 | 4.1 ± 3.8 | 5.8 ± 4.4 | 2.0 ± 1.6 | 3.8 ± 1.9 | 2.1 ± 1.0 | 3.3 ± 1.4 | 0.3 ± 0.1 |
| lodgepole pine | 0.920 ± 0.035 | 1528 ± 106 | 84.6 ± 38.8 | 4.2 ± 2.5 | 8.3 ± 7.7 | | 0.4 ± 0.2 | 0.4 ± 0.3 | 1.3 ± 1.4 | 0.3 ± 0.2 |
| Montana grass | 0.863 ± 0.062 | 1172 ± 228 | 115.3 ± 50.5 | 4.2 | 8.4 | | | | | |
| ponderosa pine | 0.920 ± 0.026 | 1589 ± 85 | 88.4 ± 30.7 | 3.2 ± 2.0 | 4.4 ± 3.7 | 1.4 ± 0.4 | 0.9 ± 1.3 | 0.4 ± 0.2 | 1.3 ± 1.0 | 0.4 ± 0.3 |
| **Rangeland** | **0.905 ± 0.043** | **1489 ± 176** | **96.4 ± 38.2** | **3.3 ± 3.1** | **3.5 ± 3.0** | **1.5 ± 1.0** | **4.6 ± 2.0** | **0.3 ± 0.2** | **2.8 ± 2.3** | **0.6 ± 0.6** |
| juniper | 0.956 | 1713 | 51 | 0.2 | 0.7 | | 2.2 | 0.2 | 0.4 | 0.1 |
| rabbitbrush | 0.935 | 1529 | 68 | 1.3 | 1.5 | 2.2 | 1.4 | 0.5 | 0.8 | 0.1 |
| sagebrush | 0.889 ± 0.041 | 1437 ± 173 | 111.2 ± 34.6 | 4.6 ± 3.1 | 4.4 ± 3.0 | 1.3 ± 1.1 | 5.7 ± 0.7 | | 4.3 ± 1.5 | 1.0 ± 0.5 |
| **Chaparral** | **0.909 ± 0.029** | **1538 ± 125** | **93.2 ± 24.1** | **2.5 ± 2.1** | **3.3 ± 2.1** | **1.4 ± 1.1** | **1.7 ± 2.2** | **0.5 ± 0.2** | **1.3 ± 1.1** | **0.3 ± 0.3** |
| ceanothus | 0.913 ± 0.012 | 1623 ± 51 | 98.3 ± 11.6 | 1.7 ± 0.4 | 1.7 ± 0.6 | 0.7 ± 0.5 | 4.3 ± 3.9 | 1.1 | 1.5 ± 0.6 | 0.3 ± 0.4 |
| chamise | 0.914 ± 0.030 | 1562 ± 112 | 86.1 ± 20.9 | 2.3 ± 1.6 | 3.4 ± 2.0 | 1.5 ± 1.2 | 1.7 ± 2.2 | 0.4 ± 0.1 | 1.1 ± 0.6 | 0.3 ± 0.3 |
| manzanita | 0.899 ± 0.030 | 1471 ± 138 | 104.4 ± 28.9 | 3.8 ± 3.6 | 4.1 ± 3.0 | 1.9 ± 1.3 | 1.3 ± 1.8 | 0.5 ± 0.1 | 1.8 ± 1.9 | 0.2 ± 0.1 |
| **Coastal plain** | **0.930 ± 0.029** | **1632 ± 150** | **78.0 ± 27.7** | **2.7 ± 1.7** | **2.6 ± 2.2** | **1.1 ± 1.2** | **4.5 ± 2.4** | **0.7 ± 0.4** | **2.0 ± 1.2** | **0.5 ± 0.5** |
| black needlerush | 0.891 ± 0.030 | 1538 ± 114 | 119.0 ± 28.3 | 5.4 ± 1.8 | 4.1 ± 1.7 | 0.7 | 3.8 ± 0.3 | | 1.8 | 0.7 |
| common reed | 0.957 ± 0.013 | 1656 ± 9 | 47.0 ± 15.6 | 1.6 ± 0.4 | 2.7 ± 0.0 | | 8.1 ± 2.1 | | 1.7 | |
| gallberry | 0.947 ± 0.004 | 1868 ± 5 | 66.0 ± 4.2 | 2.4 ± 0.2 | 1.7 ± 0.2 | 0.5 ± 0.0 | 7.3 | | 1.9 | |
| hickory | 0.933 ± 0.005 | 1583 ± 24 | 72.0 ± 4.2 | 2.7 ± 0.5 | 1.9 ± 0.1 | 0.5 ± 0.0 | | | 3.5 | |
| kudzu | 0.857 ± 0.003 | 1096 ± 35 | 116.5 ± 0.7 | 4.8 ± 1.7 | 8.4 ± 1.0 | 2.3 ± 0.2 | 6.5 ± 1.2 | | | |
| longleaf pine | 0.944 ± 0.023 | 1659 ± 78 | 60.8 ± 27.6 | 2.1 ± 0.9 | 2.7 ± 3.4 | 1.6 ± 2.2 | 3.2 ± 1.5 | 1.3 | 2.2 ± 0.8 | 0.0 ± 0.0 |
| oak | 0.943 ± 0.007 | 1622 ± 43 | 65.7 ± 3.5 | 1.7 ± 0.6 | 2.4 ± 0.4 | 0.6 ± 0.2 | 9.6 | | 3.8 | |
| palmetto | 0.933 ± 0.018 | 1678 ± 65 | 75.9 ± 19.5 | 2.3 ± 1.6 | 1.5 ± 0.8 | 0.6 ± 0.4 | 2.9 ± 1.9 | 0.5 ± 0.2 | 1.0 ± 0.8 | 0.8 ± 0.5 |
| rhododendron | 0.961 | 1783 | 46 | 1.8 | 1.2 | | 3.9 | | 2.2 | 0.1 |
| sawgrass | 0.900 ± 0.008 | 1522 ± 16 | 107.0 ± 8.5 | 3.4 ± 0.0 | 2.0 ± 0.2 | | 5.9 ± 0.6 | | 2.5 | 1.1 |
| titi | 0.942 | 1825 | 71 | 1.8 | 1.1 | | 7.6 | | | |
| turkey oak | 0.886 ± 0.006 | 1580 ± 31 | 129.5 ± 4.9 | 5.9 ± 1.2 | 4.3 ± 0.8 | 1.4 ± 0.3 | 6.3 ± 0.2 | | 5.3 | 0.7 |
| wax myrtle | 0.915 ± 0.013 | 1622 ± 61 | 95.7 ± 11.5 | 2.9 ± 0.9 | 3.7 ± 2.7 | 2.0 ± 2.3 | 3.6 ± 3.7 | 1 | 2.2 ± 0.7 | 0 |
| wire grass | 0.965 ± 0.007 | 1680 ± 9 | 43.0 ± 1.4 | 0.6 ± 0.2 | 0.4 ± 0.1 | 0.2 | 3.5 ± 0.4 | | 0.6 | |
| **Boreal forest** | **0.917 ± 0.068** | **1311 ± 325** | **70.6 ± 40.2** | **1.4 ± 0.9** | **1.7 ± 1.6** | **0.7 ± 0.6** | **3.3 ± 1.8** | **1.6 ± 1.1** | **1.8 ± 1.1** | **0.1 ± 0.1** |
| Alaskan duff | 0.867 ± 0.074 | 1034 ± 175 | 96.4 ± 43.0 | 2.3 ± 0.9 | 2.5 ± 2.7 | 1.1 ± 1.0 | 2.0 ± 0.7 | 1.0 ± 0.5 | 2.3 ± 1.2 | 0.1 ± 0.1 |
| black spruce | 0.957 ± 0.012 | 1588 ± 125 | 44.8 ± 11.2 | 0.8 ± 0.4 | 1.3 ± 0.4 | 0.5 ± 0.3 | 3.9 ± 2.0 | 3.2 | 1.1 ± 0.6 | 0.1 |
| white spruce | 0.971 | | | 1.7 | | | | | 2.5 | 0.2 |
| **Other** | **0.922 ±** | **1411 ±** | **84.4 ±** | **2.8 ± 2.8** | **2.0 ± 2.0** | **0.8 ± 0.7** | **2.2 ± 2.1** | **0.5 ± 0.1** | **0.8 ± 0.6** | **0.4 ± 0.4** |

| | | | | | | | | | | |
|---|---|---|---|---|---|---|---|---|---|---|
| | **0.035** | **82** | **29.8** | | | | | | | |
| fern | 0.943 | 1571 | 60 | 1.7 | 2.3 | 2.1 | 0.8 | 0.5 | 0.7 | 0 |
| PR mixed woods | 0.952 | | | 1.7 | 0.8 | 0.8 | | | | |
| rice straw | 0.911 ± 0.032 | 1394 ± 64 | 87.1 ± 30.3 | 3.6 ± 3.3 | 2.4 ± 2.4 | 0.5 ± 0.3 | 2.5 ± 2.2 | 0.4 ± 0.0 | 0.8 ± 0.6 | 0.5 ± 0.4 |
| sugar cane | 0.977 | | | 0.8 | 0.9 | | | | | |

1174

1175 Table 2b. Aerosol-phase emission factors by ecosystem species and group.

| **Species/Group** | **MCE** | **OC** | **EC** | **$K^+$** | **$Na^+$** | **$NH_4^+$** | **$Cl^-$** | **$NO_3^-$** | **$SO_4^{2-}$** | **$PM_{2.5}$** |
|---|---|---|---|---|---|---|---|---|---|---|
| **Montane** | **0.915 ± 0.033** | **18.4 ± 16.3** | **0.4 ± 0.8** | **0.3 ± 0.7** | **0.3 ± 0.6** | **0.3 ± 0.3** | **0.2 ± 0.2** | **0.1 ± 0.1** | **0.1 ± 0.1** | **29.4 ± 25.1** |
| Douglas fir | 0.906 ± 0.036 | 26.0 ± 14.9 | 0.36 ± 0.75 | 0.90 ± 1.22 | 0.79 ± 1.21 | 0.50 ± 0.38 | 0.31 ± 0.40 | 0.22 ± 0.19 | 0.32 ± 0.05 | 42.9 ± 22.9 |
| lodgepole pine | 0.920 ± 0.035 | 11.3 ± 15.2 | 0.45 ± 0.70 | 0.12 ± 0.19 | 0.11 ± 0.07 | 0.12 ± 0.04 | 0.13 ± 0.10 | 0.12 ± 0.05 | 0.08 ± 0.07 | 18.1 ± 23.1 |
| Montana grass | 0.863 ± 0.062 | | | | | | | | | |
| ponderosa pine | 0.920 ± 0.026 | 17.6 ± 17.0 | 0.48 ± 0.83 | 0.14 ± 0.27 | 0.17 ± 0.26 | 0.15 ± 0.14 | 0.14 ± 0.13 | 0.08 ± 0.05 | 0.06 ± 0.06 | 27.7 ± 26.0 |
| **Rangeland** | **0.905 ± 0.043** | **9.4 ± 8.1** | **1.2 ± 0.9** | **1.3 ± 0.9** | **0.4 ± 0.4** | **0.6 ± 0.5** | **1.2 ± 1.2** | **0.0 ± 0.0** | **0.2 ± 0.2** | **18.9 ± 13.9** |
| juniper | 0.956 | 0.7 | 2.7 | 0.2 | 0.02 | 0.31 | 0.11 | 0.01 | 0.08 | 4.2 |
| rabbitbrush | 0.935 | 0.5 | 1.4 | 0.67 | 0.03 | 0.23 | 0.28 | 0.06 | 0.18 | 3.4 |
| sagebrush | 0.889 ± 0.041 | 15.3 ± 1.2 | 0.63 ± 0.42 | 1.83 ± 0.67 | 0.61 ± 0.22 | 0.83 ± 0.57 | 1.82 ± 1.08 | | 0.43 | 29.0 ± 1.9 |
| **Chaparral** | **0.909 ± 0.029** | **6.6 ± 10.1** | **0.5 ± 0.4** | **0.4 ± 0.3** | **0.2 ± 0.2** | **0.5 ± 0.5** | **0.2 ± 0.1** | **0.2 ± 0.1** | **0.2 ± 0.1** | **11.6 ± 15.1** |
| ceanothus | 0.913 ± 0.012 | 3.8 ± 0.1 | 0.35 ± 0.35 | 0.60 ± 0.40 | 0.09 ± 0.09 | 0.11 | 0.38 ± 0.13 | 0.11 | 0.31 ± 0.20 | 7.8 ± 1.2 |
| chamise | 0.914 ± 0.030 | 3.2 ± 2.5 | 0.56 ± 0.48 | 0.38 ± 0.29 | 0.17 ± 0.23 | 0.50 ± 0.46 | 0.20 ± 0.14 | 0.15 ± 0.08 | 0.17 ± 0.07 | 6.5 ± 4.2 |
| manzanita | 0.899 ± 0.030 | 14.8 ± 17.3 | 0.35 ± 0.31 | 0.27 ± 0.14 | 0.16 ± 0.13 | 0.50 ± 0.70 | 0.16 ± 0.07 | 0.16 ± 0.07 | 0.16 ± 0.10 | 23.5 ± 25.9 |
| **Coastal plain** | **0.930 ± 0.029** | **12.4 ± 12.0** | **0.9 ± 1.7** | **0.8 ± 1.1** | **0.4 ± 0.5** | **0.6 ± 0.6** | **1.2 ± 1.2** | **0.1 ± 0.1** | **0.3 ± 0.2** | **23.4 ± 18.7** |
| black needlerush | 0.891 ± 0.030 | 18.3 | 0.3 | 3.19 | 2.06 | 0.57 ± 0.75 | 4.73 | | 0.49 | 38.4 |
| common reed | 0.957 ± 0.013 | 19.7 | 0.4 | 1.08 | 0.98 | 0.38 | 2.54 | | | 36.2 |
| gallberry | 0.947 ± 0.004 | 7.1 | 8.1 | 0.61 | 0.16 | | 0.16 | | 0.45 | 20.5 |
| hickory | 0.933 ± 0.005 | 7.1 | 0.3 | 0.46 | 0.24 | | 0.23 | | | 12.5 |
| kudzu | 0.857 ± 0.003 | 44.2 | 0 | 1.06 | 0.65 | 0.45 | 0.39 | | 0.99 | 70.5 |
| longleaf pine | 0.944 ± 0.023 | 23.8 ± 8.9 | 0.93 ± 0.32 | 0.24 ± 0.12 | 0.16 ± 0.06 | 0.62 ± 0.59 | 0.85 ± 0.44 | 0.02 | 0.14 ± 0.01 | 38.3 ± 13.6 |
| oak | 0.943 ± 0.007 | 10.6 | 0.4 | 0.54 | 0.28 | 0.51 | 0.23 | | 0.4 | 18.2 |
| palmetto | 0.933 ± 0.018 | 5.0 ± 6.6 | 0.47 ± 0.34 | 0.47 ± 0.45 | 0.16 ± 0.08 | 0.52 ± 0.46 | 1.27 ± 0.55 | 0.10 ± 0.10 | 0.20 ± 0.12 | 11.4 ± 10.5 |
| rhododendron | 0.961 | 2.1 | 0.2 | 0.08 | 0.03 | 0.32 | 0.08 | | 0.04 | 3.7 |
| sawgrass | 0.900 ± 0.008 | 9.2 | 1.1 | 4.69 | 0.68 | 1.32 | 3.87 | | 0.35 | 24.6 |
| titi | 0.942 | | | | | | | | | |

| | | | | | | | | | | |
|---|---|---|---|---|---|---|---|---|---|---|
| turkey oak | 0.886 ± 0.006 | 32.5 | 1.4 | 1.01 | 0.37 | 2.06 | 0.33 | | 0.23 | 52.2 |
| wax myrtle | 0.915 ± 0.013 | 6.3 ± 2.5 | 0.35 ± 0.07 | 0.62 ± 0.06 | 0.28 ± 0.01 | 0.06 | 0.95 ± 0.25 | 0.08 | 0.26 ± 0.13 | 12.2 ± 4.0 |
| wire grass | 0.965 ± 0.007 | 3.5 | 0.3 | 0.19 | 0.17 | 0.87 | 0.18 | 0.1 | | 6.4 |
| **Boreal forest** | **0.917 ± 0.068** | **7.8 ± 7.2** | **0.2 ± 0.4** | **0.2 ± 0.1** | **0.2 ± 0.4** | **0.5 ± 0.8** | **0.1 ± 0.2** | **0.1 ± 0.1** | **0.0 ± 0.0** | **12.7 ± 11.3** |
| Alaskan duff | 0.867 ± 0.074 | 10.2 ± 10.0 | 0.00 ± 0.00 | 0.15 ± 0.19 | 0.32 ± 0.54 | 0.26 | 0.14 ± 0.22 | 0.04 ± 0.01 | 0.05 ± 0.01 | 16.1 ± 15.9 |
| black spruce | 0.957 ± 0.012 | 6.2 ± 2.8 | 0.60 ± 0.46 | 0.15 ± 0.10 | 0.09 ± 0.05 | 0.84 ± 1.11 | 0.10 ± 0.07 | 0.16 | 0.04 | 10.4 ± 4.2 |
| white spruce | 0.971 | 3.5 | 0 | 0.16 | 0.08 | 0.01 | 0.31 | 0.1 | | 5.9 |
| **Other** | **0.922 ± 0.035** | **5.6 ± 3.5** | **0.1 ± 0.1** | **0.5 ± 0.3** | **0.1 ± 0.1** | **0.3 ± 0.6** | **1.0 ± 0.5** | **0.1 ± 0.0** | **0.1 ± 0.1** | **10.2 ± 6.6** |
| fern | 0.943 | 2.2 | 0.1 | 0.06 | 0.01 | 0.1 | 0.01 | 0.04 | 0.04 | 3.9 |
| PR mixed woods | 0.952 | | | | | 0.09 | | 0.01 | | |
| rice straw | 0.911 ± 0.032 | 6.2 ± 3.5 | 0.08 ± 0.15 | 0.57 ± 0.18 | 0.14 ± 0.13 | 0.44 ± 0.72 | 1.19 ± 0.15 | 0.08 ± 0.02 | 0.12 ± 0.09 | 11.8 ± 6.5 |
| sugar cane | 0.977 | | | | | 0.1 | | 0.07 | | |

1176

1177 FIGURE CAPTIONS

1178 Figure 1. Schematic of the US Forest Service Fire Sciences Laboratory combustion facility,
1179 located in Missoula, Montana. Image is to scale. The locations of the fuel bed and of the
1180 sampling ports during stack and chamber burns are indicated.

1181 Figure 2. Scatter plots comparing elemental carbon (EC) concentrations normalized by total
1182 aerosol carbon (TC) concentrations, for each thermal optical analysis protocol and/or filter
1183 sampler used during FLAME chamber burns. The dashed black line is the 1:1 line and the two
1184 dashed gray lines are the 1:2 and 2:1 lines.

1185 Figure 3. Organic carbon (OC) concentrations measured on the back IMPROVE quartz filter
1186 normalized by OC measured on the front IMPROVE quartz filter, as a function of front filter
1187 OC. Chamber burns only.

1188 Figure 4. Fire-integrated modified combustion efficiency plotted as a function of fuel moisture
1189 (in dry weight %).

1190 Figure 5. Gravimetrically-determined mass concentrations of particles with aerodynamic
1191 diameters less than 10 μm ($PM_{10}$) compared to gravimetrically-determined mass concentrations
1192 of particles with diameters less than 2.5 μm ($PM_{2.5}$) for IMPROVE filter samples obtained
1193 during chamber burns. Dashed line is the 1:1 line. Solid line gives the linear regression of $PM_{10}$
1194 mass onto $PM_{2.5}$ mass, forced through the origin, for all but the highest three concentration
1195 samples.

1196 Figure 6. Carbon mass consumed versus carbon mass emitted during FLAME. Carbon mass
1197 consumed was calculated assuming the residual mass had zero water content. Carbon mass

emitted consists of the sum of carbon monoxide, carbon dioxide, methane, $C_{2-4}$ hydrocarbons, and particulate carbon. Points are shaded by fuel moisture to indicate samples where the assumption is less likely to be valid. Circles indicate stack burns and triangles indicate chamber burns.

Figure 7. Fire-integrated emission factors for hydrocarbon gas species calculated from canister gas chromatography measurements as a function of fire-integrated modified combustion efficiency (MCE), for all tested fuels. Black lines indicate the linear least-squares regression of the emission factors onto MCE.

Figure 8. Elemental-to-total aerosol carbon (EC/TC) ratios observed for emissions from (a) ponderosa pine and (b) chaparral and desert shrub fuels, versus fire-integrated modified combustion efficiency (MCE). Ponderosa pine data include needle, branch, needles and branches, needle litter and duff burns. Samples collected during only flaming (high MCE) and smoldering (low MCE) combustion of ponderosa pine needles are indicated by the filled circles; all others are fire-integrated. Previously measured ratios from selected studies are also shown.

Figure 9. Fire-integrated aerosol emission factors (EF) as a function of fire-integrated modified combustion efficiency (MCE) for: a) organic carbon (OC); b) elemental carbon (EC); c) total aerosol carbon (TC); d) chloride; e) potassium; f) total inorganic aerosol species and g) reconstructed PM2.5. Black lines indicate the linear regression of EF onto MCE with coefficients and coefficient of variation indicated on the plot for each species.

Figure 10. Molar ratios of $NH_3$-to-$NO_X$ emissions as a function of fire-integrated modified combustion efficiency (MCE) during FLAME and as reported for several other biomass burning field and laboratory experiments, as indicated in the legend. FLAME data are shaded to reflect

1220 the magnitude of the $NO_X$ measurement, and therefore reflect the confidence in the measured
1221 ratio. The dashed line indicates the fit provided by *Goode et al.* [2000] for several sets of
1222 laboratory and field biomass burning measurements. Note that this figure is truncated to better
1223 illustrate the majority of $NH_3/NO_X$ data from our study and the literature. A maximum $NH_3$:$NO_X$
1224 ratio of ~12 at an MCE of 0.82 was reported by *Christian et al.* [2003].

1225 FIGURES

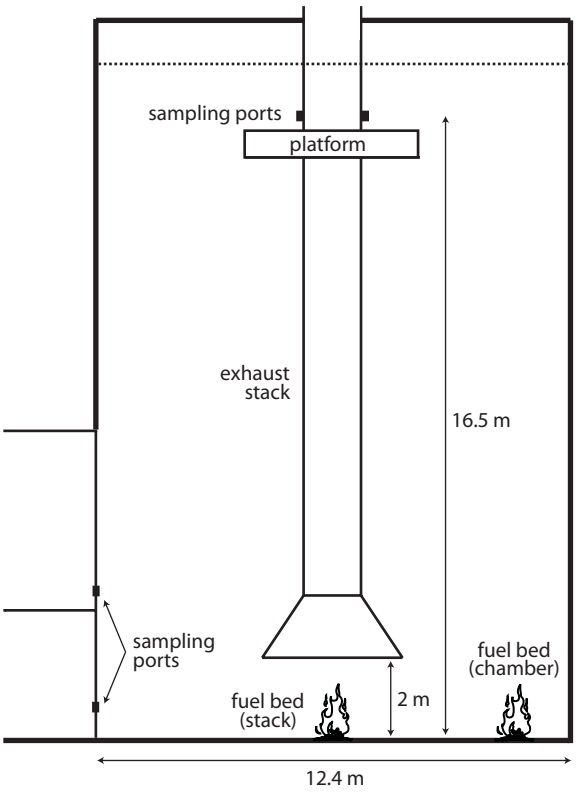


1226

1227 Figure 1 Schematic of the US Forest Service Fire Sciences Laboratory combustion facility,
1228 located in Missoula, Montana. Image is to scale. The locations of the fuel bed and of the
1229 sampling ports during stack and chamber burns are indicated.

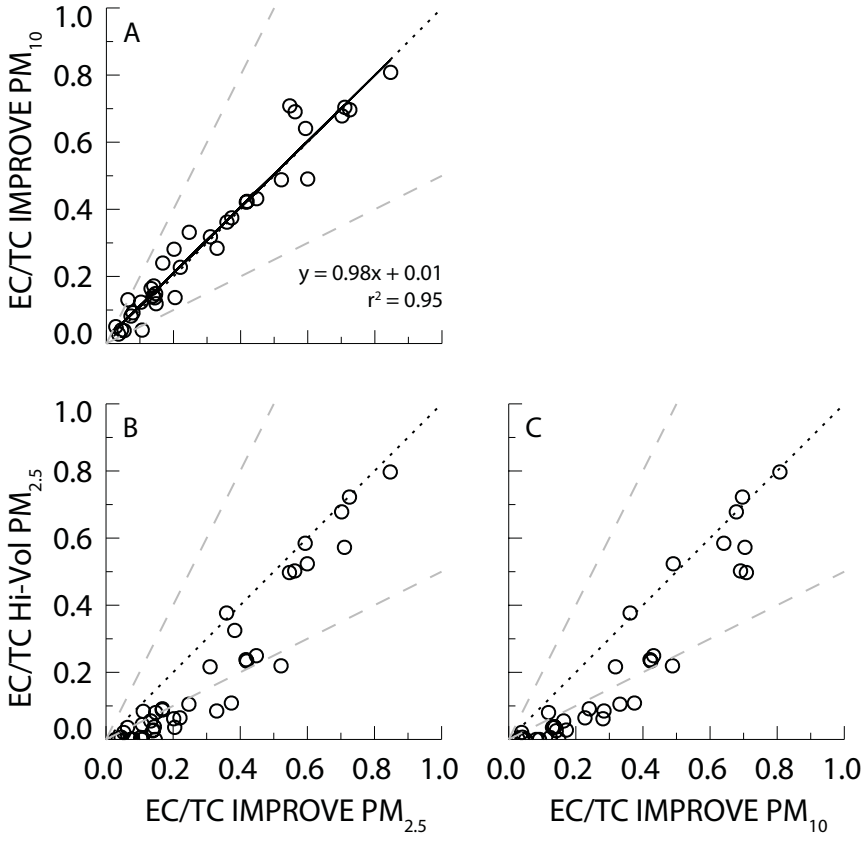


Figure 2 Scatter plots comparing elemental carbon (EC) concentrations normalized by total aerosol carbon (TC) concentrations, for each thermal optical analysis protocol and/or filter sampler used during FLAME chamber burns. The dashed black line is the 1:1 line and the two dashed gray lines are the 1:2 and 2:1 lines.

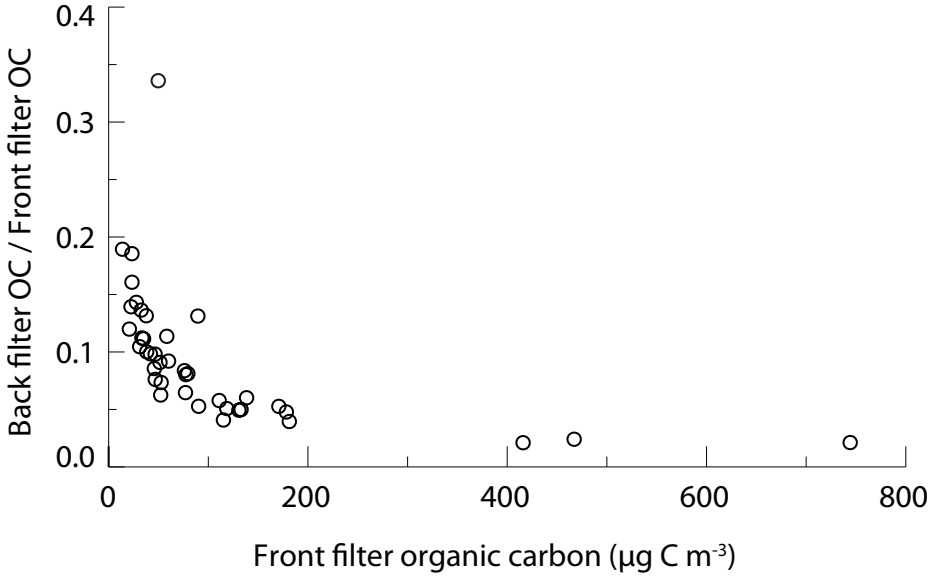

1236 Figure 3 Organic carbon (OC) concentrations measured on the back IMPROVE quartz filter
1237 normalized by OC measured on the front IMPROVE quartz filter, as a function of front filter
1238 OC. Chamber burns only.

1239

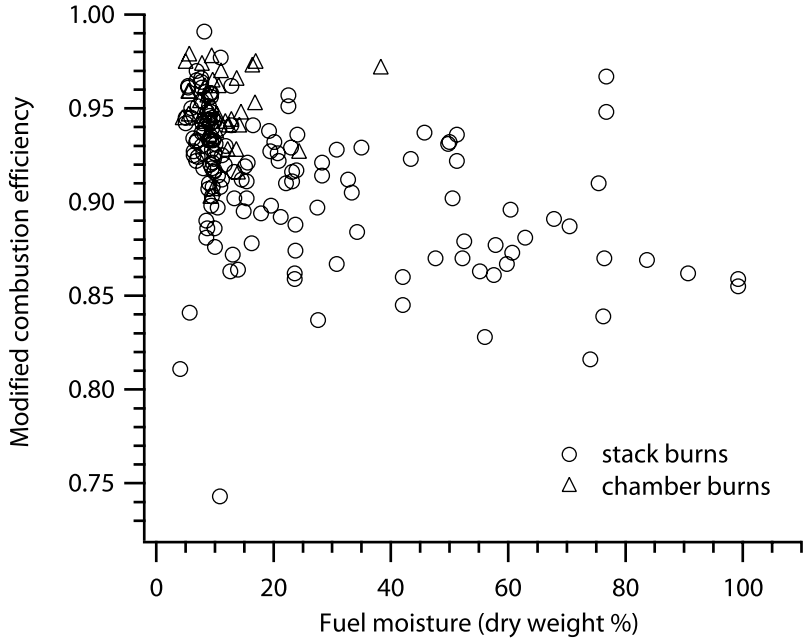


1240

1241 Figure 4 Fire-integrated modified combustion efficiency plotted as a function of fuel moisture (in
1242 dry weight %).

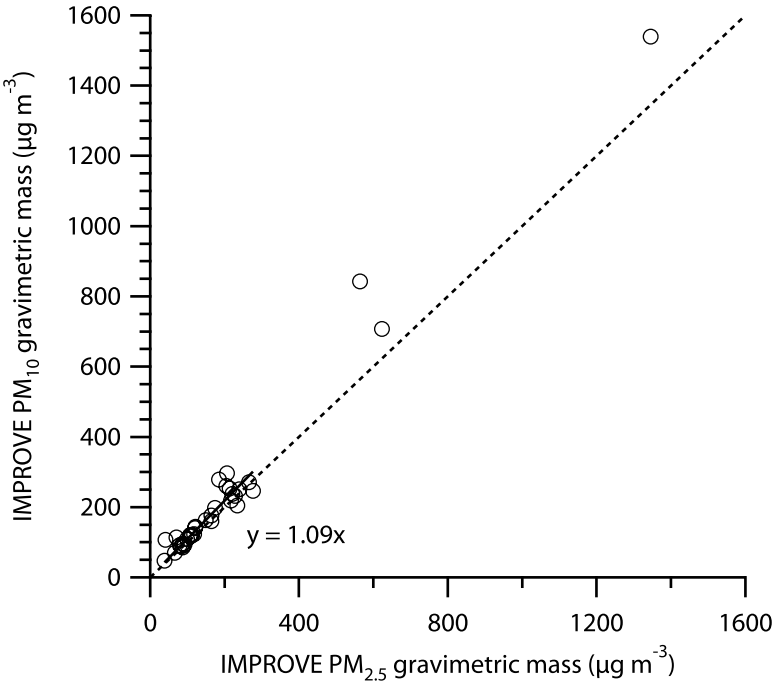


Figure 5 Gravimetrically-determined mass concentrations of particles with aerodynamic diameters less than 10 µm ($PM_{10}$) compared to gravimetrically-determined mass concentrations of particles with diameters less than 2.5 µm ($PM_{2.5}$) for IMPROVE filter samples obtained during chamber burns. Dashed line is the 1:1 line. Solid line gives the linear regression of $PM_{10}$ mass onto $PM_{2.5}$ mass, forced through the origin, for all but the highest three concentration samples.

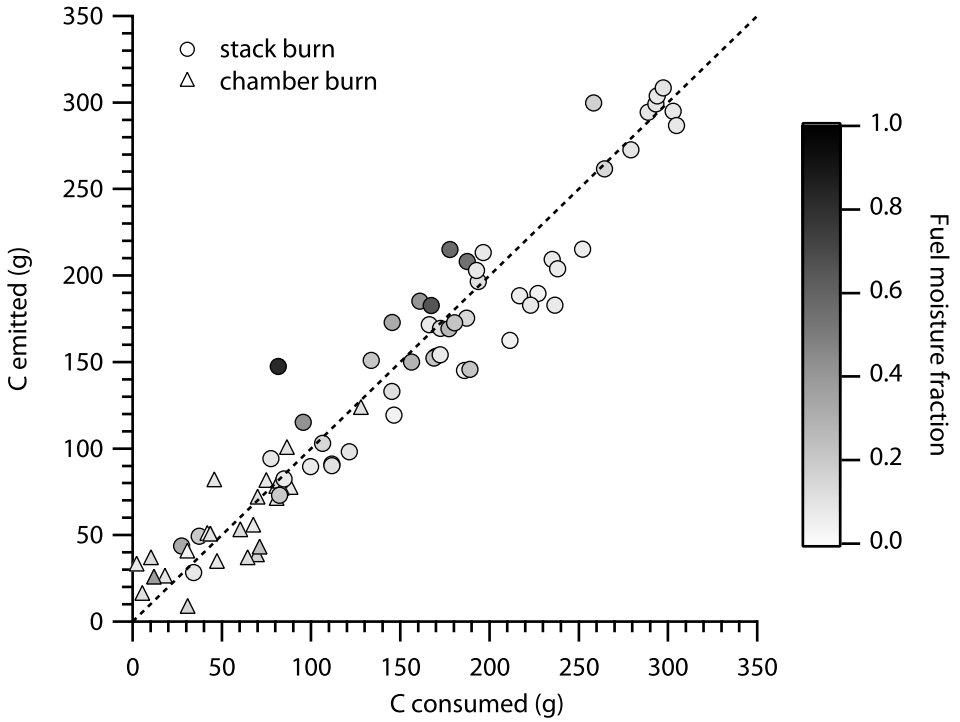


Figure 6 Carbon mass consumed versus carbon mass emitted during FLAME. Carbon mass consumed was calculated assuming the residual mass had zero water content. Carbon mass emitted consists of the sum of carbon monoxide, carbon dioxide, methane, $C_{2-4}$ hydrocarbons, and particulate carbon. Points are shaded by fuel moisture to indicate samples where the assumption is less likely to be valid. Circles indicate stack burns and triangles indicate chamber burns.

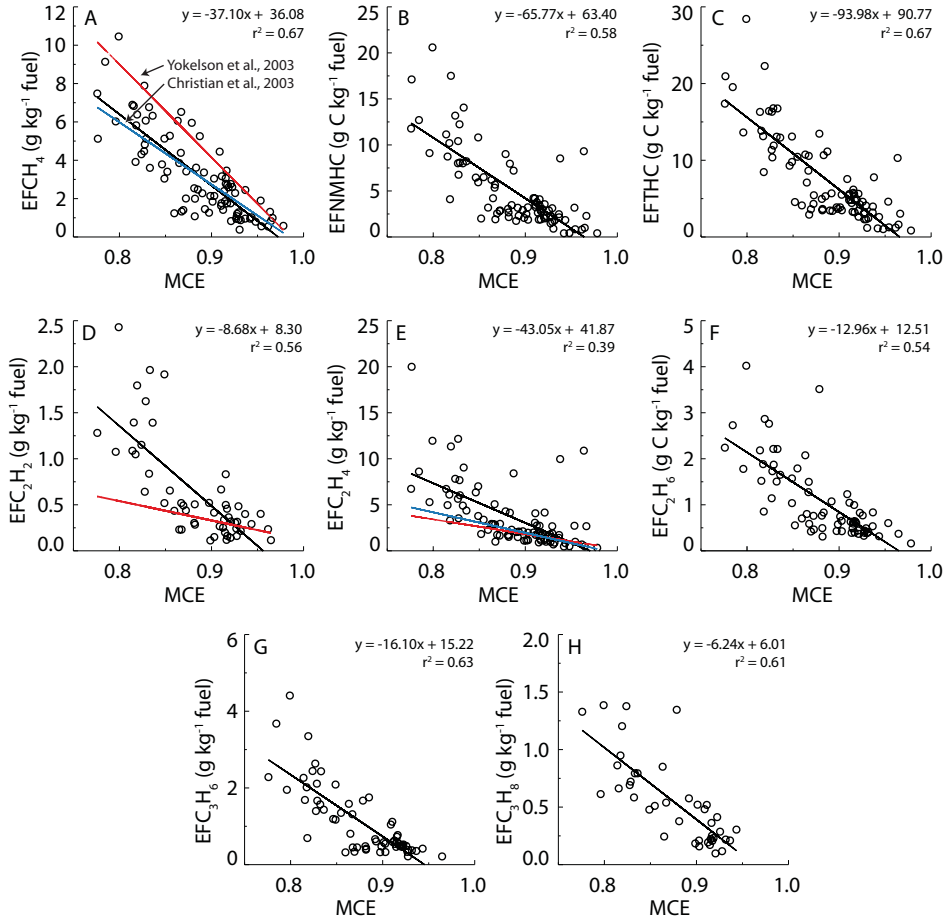


Figure 7 Fire-integrated emission factors for hydrocarbon gas species calculated from canister gas chromatography measurements as a function of fire-integrated modified combustion efficiency (MCE), for all tested fuels. Black lines indicate the linear least-squares regression of the emission factors onto MCE.

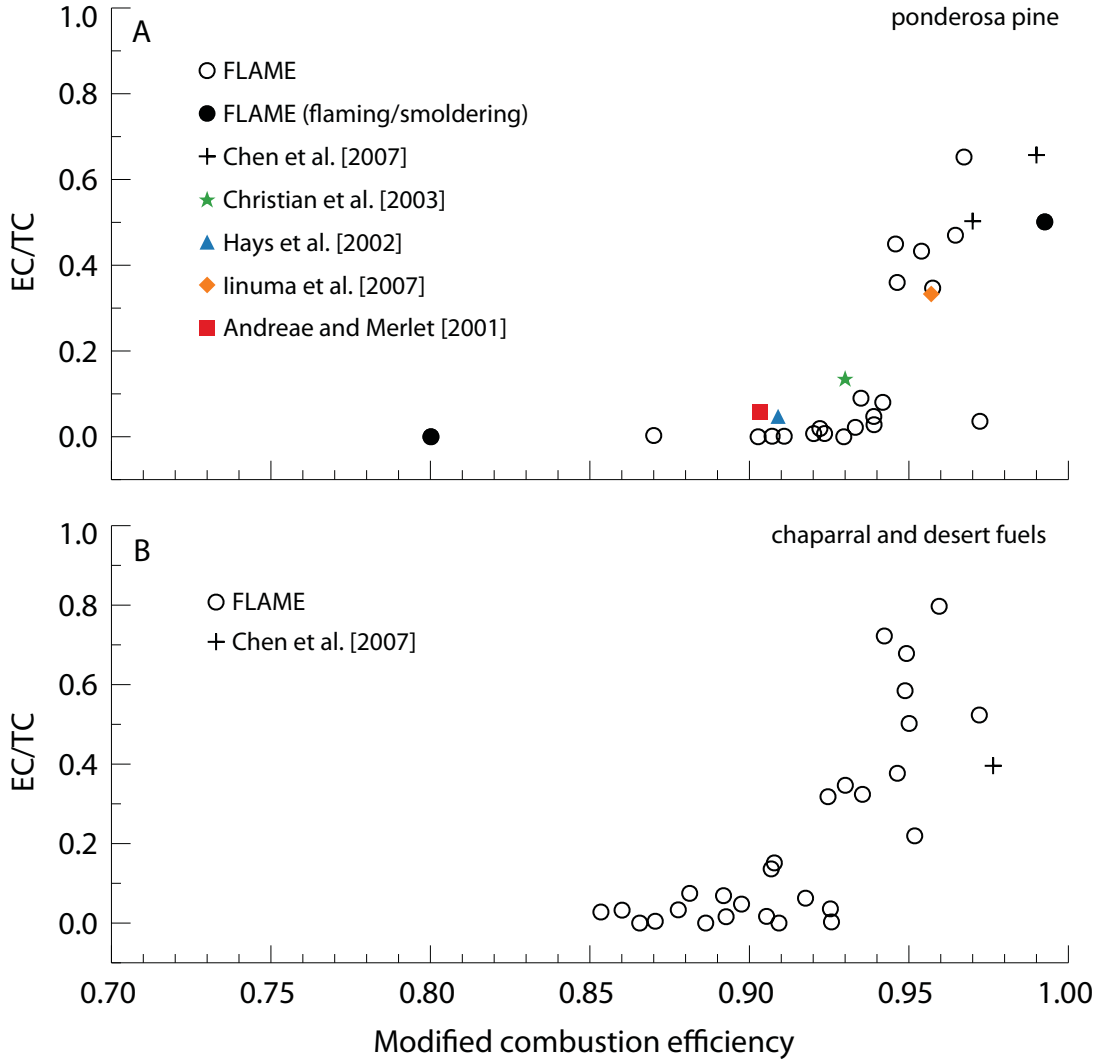


Figure 8 Elemental-to-total aerosol carbon (EC/TC) ratios observed for emissions from (a) ponderosa pine and (b) chaparral and desert shrub fuels, versus fire-integrated modified combustion efficiency (MCE). Ponderosa pine data include needle, branch, needles and branches, needle litter and duff burns. Samples collected during only flaming (high MCE) and smoldering (low MCE) combustion of ponderosa pine needles are indicated by the filled circles; all others are fire-integrated. Previously measured ratios from selected studies are also shown.

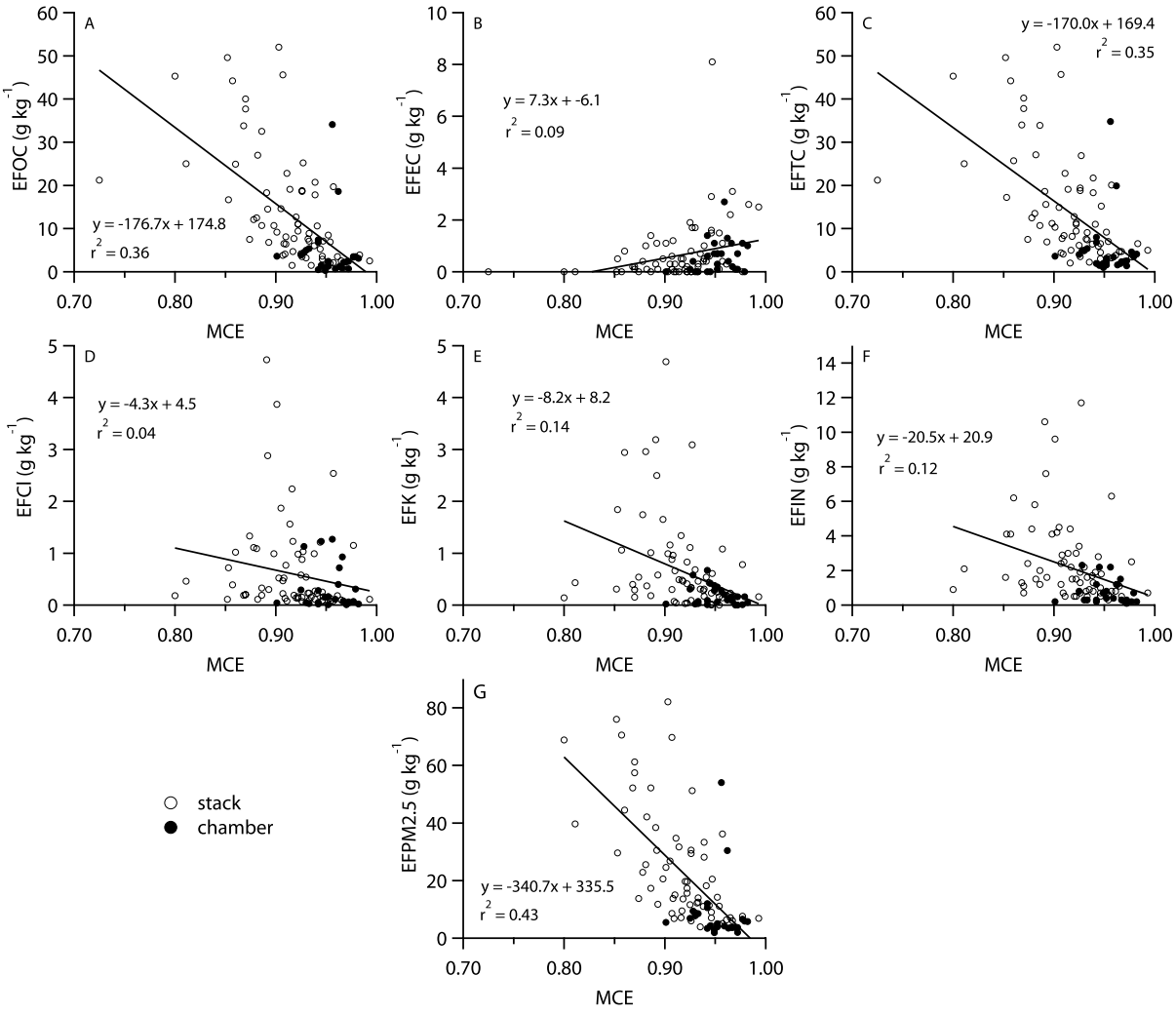


1273

1274 Figure 9 Fire-integrated aerosol emission factors (EF) as a function of fire-integrated modified
1275 combustion efficiency (MCE) for: a) organic carbon (OC); b) elemental carbon (EC); c) total
1276 aerosol carbon (TC); d) chloride; e) potassium; f) total inorganic aerosol species and g)
1277 reconstructed PM2.5. Black lines indicate the linear regression of EF onto MCE with coefficients
1278 and coefficient of variation indicated on the plot for each species.

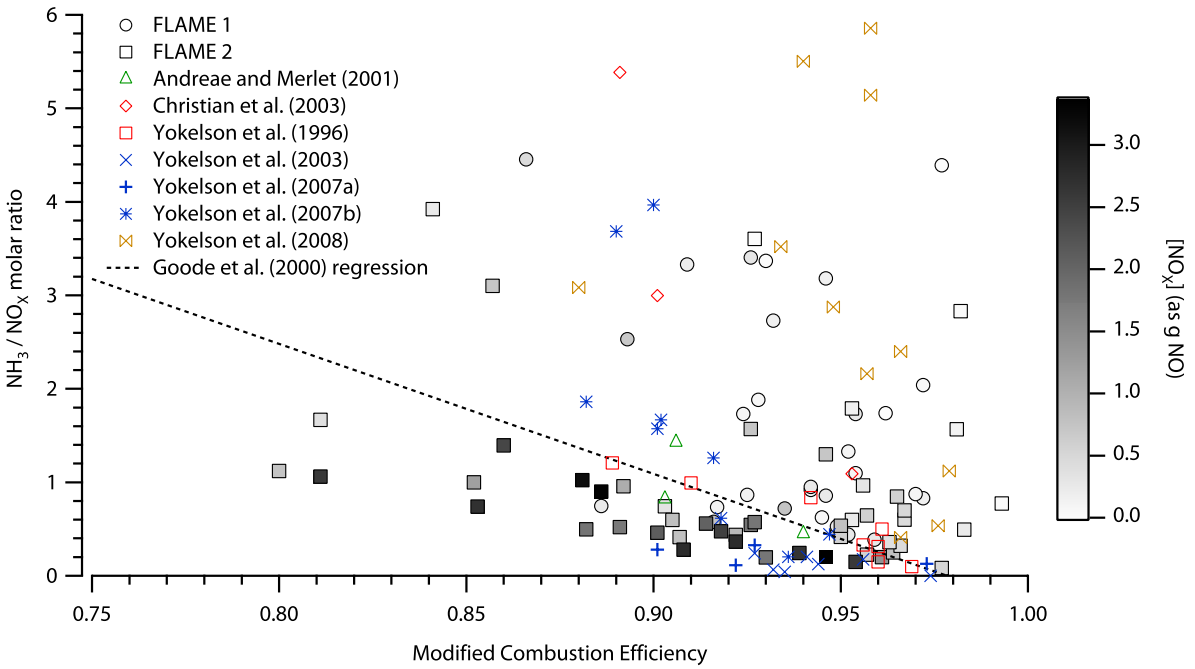


1279

1280 Figure 10 Molar ratios of $NH_3$-to-$NO_X$ emissions as a function of fire-integrated modified
1281 combustion efficiency (MCE) during FLAME and as reported for several other biomass burning
1282 field and laboratory experiments, as indicated in the legend. FLAME data are shaded to reflect
1283 the magnitude of the $NO_X$ measurement, and therefore reflect the confidence in the measured
1284 ratio. The dashed line indicates the fit provided by *Goode et al.* [2000] for several sets of
1285 laboratory and field biomass burning measurements. Note that this figure is truncated to better
1286 illustrate the majority of $NH_3/NO_X$ data from our study and the literature. A maximum $NH_3$:$NO_X$
1287 ratio of ~12 at an MCE of 0.82 was reported by *Christian et al.* [2003].